

FIT4MEDROB

D8.2.1

RTA2 - SENSORS, ACTUATORS AND ENERGY STORAGE SYSTEMS #1

Piano Nazionale Complementare (PNC) – Decreto Direttoriale n. 931 del 6 giugno 2022 – Avviso per la concessione di finanziamenti destinati ad iniziative di ricerca per tecnologie e percorsi innovativi in ambito sanitario e assistenziale

Initiative identifier: PNC0000007

Start date: 01/12/2022

Duration: 44 months

Website: www.fit4medrob.it

MLs: Loredana Zollo (UCBM), Fanny Ficuciello (UNINA)

ALs: Andrea Orlandini (CNR), Fabrizio Dabbene (CNR), Fanny Ficuciello (UNINA), Gionata Salvietti (UNISI), Loretta L. del Mercato (CNR), Paolo Netti (UNINA), Laura Pastorino (UNIGE)

Due date of deliverable: 30/11/2023

Actual submission date: 20/09/2024

Version: 1.1

DISSEMINATION LEVEL OF DELIVERABLE

PU	Public, fully open, e.g. web	X
CO	Confidential, restricted under conditions set out in Partners Agreement	



Ministero
dell'Università
e della Ricerca



Italiadomani
PIANO NAZIONALE
DI RIPRESA E RESILIENZA



PNC

Piano nazionale per gli investimenti
complementari al PNRR
Ministero dell'Università e della Ricerca

HISTORY OF CHANGES

VERSION	SUBMISSION DATE	CHANGES
1.0	30/11/2023	First version
1.1	20/09/2024	Introduction modified following reviewers' suggestions.



Ministero
dell'Università
e della Ricerca



Italiadomani
PIANO NAZIONALE
DI RIPRESA E RESILIENZA



PNC

Piano nazionale per gli investimenti
complementari al PNRR
Ministero dell'Università e della Ricerca

TABLE OF CONTENTS

History of Changes.....	2
1 Executive Summary	4
1.1 SENS4SOFTROB (NOVEL SENSING SYSTEMS FOR WEARABLE SOFT ROBOTS)	7
1.1.1 Research team.....	7
1.1.2 Introduction	7
1.1.3 Proprioception and device sensing	8
1.1.4 Human sensing for controlling the device	10
1.1.5 Interaction with the environment.....	12
1.2 CATE (Compliant AcTuation for wEarable robots).....	14
1.2.1 Research team.....	14
1.2.2 Introduction	14
1.2.3 Research activities and achievements.....	15
1.2.4 Analysis of the state of the art on compliant components for rotary SEAs.....	15
1.3 TEST DEM (TAILORED ENERGY STORAGE DESIGN, EXPERIMENTATION AND MODELLING)	21
1.3.1 Research team.....	21
1.3.2 Introduction	21
1.3.3 Critical analysis of available storage devices and evaluation of possible solutions for cooling and design optimization.....	21
1.3.4 Selection of case studies and identification of main requirements for the specific applications.....	27
References	35

1 EXECUTIVE SUMMARY

Mission 3 is devoted to support **frontier research topics** pertaining to physical and computational aspects of robot *bodies*, robot intelligence, and interfaces with the patient. Seven research topics (RTa1...RTa4, RTb1..RTb3) are articulated in 19 sub-projects, running in parallel and covering complementary enabling technologies in the field of robotics and biorobotics.

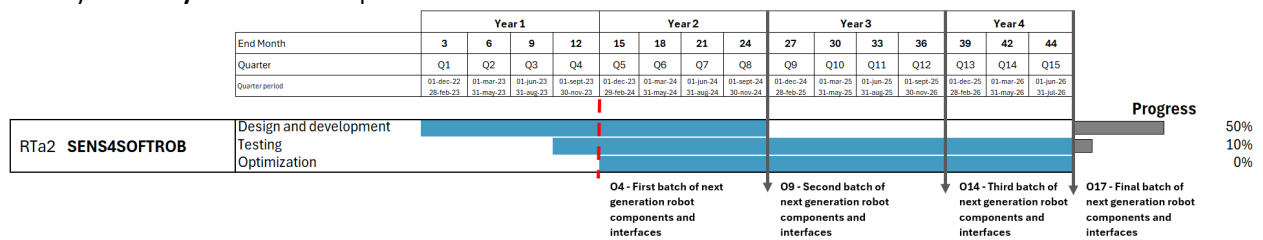
Research Topic a2 is dedicated to the development of new sensors, actuators and Energy Storage Systems with the ultimate goal of gaining insights into possible applications of such technologies for robot prototypes. RTa2 comprises three sub-projects addressing complementary research: **Sens4SoftRob** (novel sensing systems for wearable soft robots), **CATE** (compliant actuation for wearable robots) and **TEST-DEM** (tailored energy storage design, experimentation and modeling).

This document reports the activities carried out within RTa2 in the first year of Fit4MedRob. Sens4SoftRob focused on: (i) the progress concerning the proprioception and sensing of a soft robot device, (ii) preliminary results obtained for using bio-signal for controlling the robot, and (iii) improving the human interaction with the environment by exploiting exteroceptive measurements. CATE focused on the overall process for design, development, integration and testing of virtual prototypes and on the development of Computer-Aided frameworks for optimal design of compliant elements. TEST-DEM focused on the analysis and comparison of available storage devices, with the associated optimization and experimental testing solutions, and of bio-robotic applications available in the scientific literature for the identification of their main power/energy requirements.

As per the proposal, the expected impact of Mission 3 is a new wave of technologies (proofs of concept or proofs of viability) and of knowledge, at the basic or component level, to become key enabling components of future healthcare and personal care robots.

SENS4SOFTROB progress

The timeline of the project SENS4SOFTROB is represented in the Gantt chart below. Specifically, “Design and Development” is referred to sensorizing passive joints of robotic extra fingers for enhanced proprioception. Then, an edge-AI electronic device to acquire biomedical signals, with particular reference to dataset and data pre-processing activities is in development. The last activity for this sub-project is related to heterogeneous sensorimotor representation of the space surrounding a robot. The **“Design and Development”** phase is **50%** advanced compared to the planned Gantt. We have preliminary versions of the prototypes that are going to start the testing phase. So that, the **“Testing”** phase is starting with the **10%** of the total time spent to setup the tests. The **“Optimization”** activity has **not yet started** as reported in the Gantt.



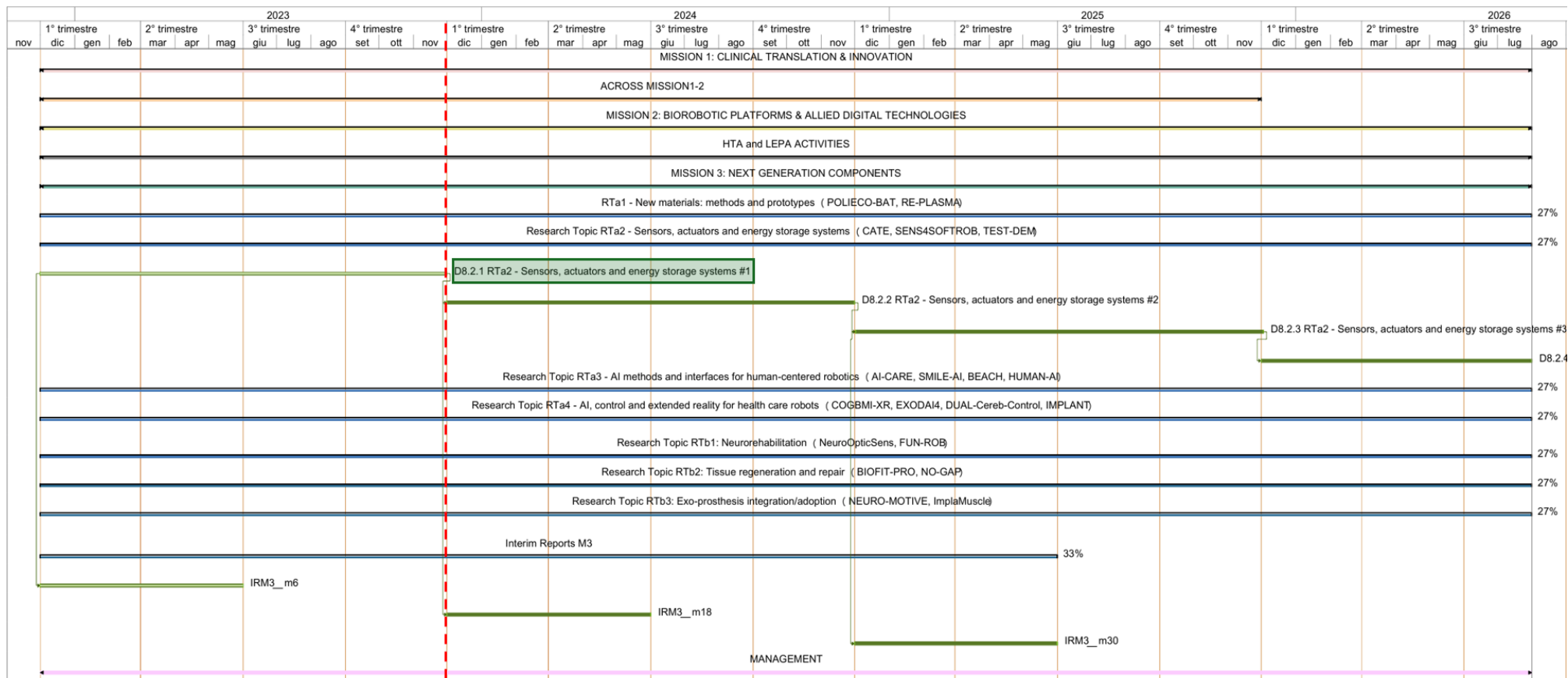
There are no deviations on the original plan and the research is progressing as originally foreseen.

CATE progress

The timeline of the project CATE is represented in the Gantt chart below. Specifically, “Design and Development” is mainly focusing on the analysis of state-of-the-art components and novel solutions for Serial Elastic Actuators and on the design of a compliant trans-humeral prosthetic device covering the elbow, wrist, and hand, with a total of 7 degrees of actuation (DOA). The **“Design and Development”** phase is **45%** advanced compared to the planned Gantt. We have preliminary versions of the prototypes that will start the testing phase.

The **“Testing”** and **“Optimization”** activities have **not yet started** as reported in the Gantt.

There are no deviations on the original plan and the research is progressing as originally foreseen.



1.1 SENS4SOFTROB (NOVEL SENSING SYSTEMS FOR WEARABLE SOFT ROBOTS)

1.1.1 Research team

The research team involved in this project encompasses 6 research units, namely the University of Naples (UNINA), the University of Siena (UNISI), the University of Modena and Reggio (UNIMORE), the University of Genoa (UNIGE), the Institute for Microelectronics and Microsystems, CNR of Lecce (CNR-IMM) and finally the Institute of Electronics and of Information and Communications engineering, CNR (CNR-IEIIT).

The composition of the research team is detailed in the following **Table 1**.

Table 1 - Research team.

UNINA	Giovanni Breglio, Antonello Cutolo, Michele Riccio
UNISI	Ada Fort, Agnese Magnani, Gionata Salvietti, Tommaso Lisini Baldi, Elia Landi
UNIMORE	Luigi Rovati, Alberto Ferrari, Giovanni Gibertoni
UNIGE	Silvio P. Sabatini, Giorgio Cannata, Francesco Grella, Francesco Giovinazzo, Marco Staiano
CNR-IMM LECCE	Luca Francioso
CNR-IEIIT	Elisabetta Punta

1.1.2 Introduction

Soft robots exhibit distinctive characteristics when compared to their conventional counterparts. Traditional robot structures are typically fabricated from high-stiffness materials, such as steel, aluminium, titanium, and stainless steel. These components are shaped using mechanical machining tools, including milling machines, lathes, and computerized numerical control (CNC) machines, and are subsequently assembled through mechanical means.

In stark contrast, soft robots employ hyperelastic materials for their body and moving parts, including polymers, rubber, silicone, and other flexible materials. These materials are shaped through the use of three-dimensional (3D) printers or moulds.

Soft robots inherently prioritize safety and are exceptionally versatile, capable of performing a wide range of tasks, such as functioning as universal grippers. They harness the unique property of their elastic bodies to adapt passively to the objects they interact with. As a result, they find diverse applications in contexts like safe human-robot interactions, delicate object manipulation, and the traversal of challenging and unstructured environments. Their utility is particularly pronounced in assistive and rehabilitation scenarios.

Soft robots can be significantly improved by incorporating proprioceptive and tactile sensing capabilities, encompassing measurements of strain, pressure, bending, twisting, and other physical parameters. Furthermore, optimizing their interaction with the human wearing the robot and the surrounding environment is pivotal for the successful implementation of more precise and compliant control strategies enabling the execution of complex tasks such as grasping, manipulation, locomotion, and exploration.

Sensing capabilities have been a focal point in soft robotics research since the inception of this field [1]. Over time, notable advancements have been achieved, capitalizing on significant progress in the production of soft material structures, the fabrication techniques for flexible and stretchable sensors, and the development of flexible electronics. However, it is worth noting that within the domain of soft robotics, the field of sensing is still in its nascent stages and relatively less advanced in comparison to the areas of actuation and structural reinforcement [[2] and the reference therein].

The Sens4SoftRob project aims at developing new sensing systems and solutions for the enhancement of soft robot performance, considering the increase of proprioception capability, of interaction with the man wearing the robot and with the environment. In what follows we detail: i) the progresses concerning the proprioception and sensing of the device, ii) preliminary results obtained for using biosignal for controlling the robot, and iii) improving the human interaction with the environment by exploiting exteroceptive measurements.

1.1.3 Proprioception and device sensing

As mentioned earlier, perception plays a crucial role in enabling robots to safely navigate unfamiliar environments and interact with both humans and their surroundings. When dealing with proprioception, soft robots introduce distinctive challenges not encountered by their rigid counterparts. These challenges arise from the vast degrees of freedom (DOFs) inherent in soft robots and their susceptibility to deformation caused by both internal actuation and external forces. Therefore, the task of sensorizing soft robots for proprioception becomes particularly significant, given the inherent complexity of accurately predicting or modelling their responses under specific driving conditions. This complexity is further exacerbated by the intricate nature of the hyperelastic materials frequently employed, which exhibit characteristics such as nonlinearity, hysteresis, viscoelastic effects, substantial strain, and deformations [3].

State of the art

There are many challenges for implementing mechanically perceptive soft robots, a major one is that there is no clear distinction between proprioception and tactile sensing when designing a sensing system for soft robots. Sensing has been investigated since the birth of soft robots, [4] with a major interest in sensing exploiting soft materials or structures, and flexible electronics [1], [2].

A variety of 'soft' sensing technologies have been proposed [2], [5], but there is still a gap to effectively utilize them in soft robots for practical applications. With specific regard to proprioceptive sensors, specifically aiming at measuring the curvature of robot components, those proposed in the literature are based on 'soft technologies' including low modulus (<1 MPa) elastomers with liquid-phase material-filled channels and resistive, capacitive or inductive reading [1 and its references] stretchable conductive materials, elastomeric conductors, which consist of elastomers loaded with conductive micro/nano particles/wires such as silver nanowires, silver particles, carbon nanotubes, and graphene, piezoelectric polymers and so on [2]. The limitations of these sensors in terms of lifespan and reliability have been noted in previous studies.

As far as the tactile sensing is concerned, in the past decade, significant progress has been made in the development of flexible, thin electronic skins, particularly in the context of tactile sensing. This progress has been made possible by advancements in printing techniques, flexible organic electronics, and the utilization of advanced materials. Some notable examples include ultralightweight tactile sensing arrays with integrated organic electronics and fully printed flexible tactile skins capable of tri-axis force and temperature sensing. Comprehensive reviews of electronic skins can be found in relevant literature [1]. A range of ultrathin, flexible electronic skins has found applications in wearable and biomedical systems.

Despite the common assertion that the deformable nature of soft robots or wearable robot components limits the use of conventional rigid sensors like encoders, strain gauges etc., accurate designs and the use of multiple materials or composites can adapt some of these established technologies to provide accurate and reliable measurements.

For instance, some researchers have already integrated flexible tactile sensors or sensing skins with integrated rigid electronics into traditional robotic systems. Notwithstanding some drawbacks due to the different mechanical behaviour of these components with respect to the soft structure, the materials, electronics, and fabrication technologies used in developing such thin skins have superior reproducibility and performance.

In recent times, researchers have ventured into implementing combined proprioception and tactile sensing systems in soft robots. For instance, some research groups [6][7], embedded optical waveguides in robots as strain and pressure sensors. This technology can enable the simultaneous detection of the bending angle of flexible parts (proprioception) and the sensing of contact force at mobile component ends (tactile sensing). While these sensing technology and associated electronics may be bulky and expensive the research demonstrates the potential for significantly enhancing the capabilities of soft robotic hands by enabling mechanical perception.

Objective and activity

In the context of this subproject, concerning proprioception and tactile sensing we selected as a first case study the sixth finger developed at the university of Siena [8], with the aim of enhancing its sensorization. The activity will proceed with the empowerment of proprioception and in particular with sensors for measuring bending of the soft joints. This goal has also a vast application since bending is the predominant deformation mode in soft robotics.



Figure 1 - Sixth finger developed at UNISI.

Besides analysing and testing solutions based on promising soft materials as hydrogels for instance [5], at first, as an alternative to the 'soft sensing', we aim at the application of strain gauges based on thin films on polymeric substrates, properly designed and mounted, to yield reliable results while minimizing issues related to hysteresis and low reproducibility of individual sensors.

The concept involves the creation of layered structures specifically designed for soft joints. These structures incorporate thin flexible substrates realized with materials that guarantee optimal adherence to both the joint's base material and the strain gauges. The substrate thickness is carefully chosen to accommodate limited strain, aligning seamlessly with the sensor's full range of capabilities.

This solution allows for the use of assessed thin film technologies and traditional structures for strain sensors characterized by very high reproducibility and accuracy. In fact, the fabrication of 'soft' components employs various methods, such as mask deposition of conductors [1] and direct 3D printing of conductive materials [1], all of which provide moderate accuracy and reproducibility, not comparable to those achieved with thin film deposition technology. With the approach followed in this first case study, the source of uncertainty shifts from sensor fabrication to sensor positioning and coupling with the soft material.

Achievements

To address this issue, preliminary tests have been conducted in this part of the project. A possible solution has been designed, suitable for embedding in soft components created through moulding and has been applied to silicone rubber joints of a supernumerary finger developed at UNISI.

Three different prototypes were built exploiting commercial C4A encapsulated Constantan alloy gauges (Vishay Precision Group, Inc.) with linear range of 3%. This involved burying a couple of devices at the same depth from the opposite surfaces of a joint and then mounting them in a half bridge configuration. The depth was chosen after a simulation study.

Two prototypes were developed by embedding the devices within the silicone rubber soft joint structure at two distinct depths, whereas a third one was obtained by gluing with cyanoacrylate two strain gauges at the two surfaces of a thin layer of butyl rubber and then burying the as obtained structure in the soft joint. A front-end electronic interface was designed to read-out the half-bridge output and acquire the voltage output. The prototypes were tested by means of a self-produced automatic test bench able to induce a known bending angle to the joint and then measuring the strain. The initial two prototypes exhibit noticeable hysteresis in their behavior, while the third one demonstrates a reproducible response with low hysteresis. (the output shown in **Figure 2**), from the preliminary results, an error of a few degrees was estimated. Moreover, the test bench allowed for continuous monitoring of the bending angle, which allowed for dynamic tests, during which a phalanx of the finger was actuated with a tendon.

Exploiting the results obtained, the design of an array of flexible thin film strain gauges was defined. It consists of flexible substrates (like Kapton) supporting a patterned strain-sensitive layer, such as Karma alloys. The use of thin films sensing layer favours the reduction of the sensor sizes, making negligible the mechanical stiffness of the strain gauges and enhancing the device performance. In addition, the strain transferability and the response time of thin-film strain gauge are excellent, so they result more suitable for dynamic strain tests. The system will be entirely fabricated by CNR-IMM of Lecce Unit, where lithographic and thin films deposition equipment is available in a controlled environment (cleanroom facility) for the realization of devices with high resolution quality.

The production of the strain gauges array is actually ongoing in cooperation with CNR-IMM partner, that can offer microfabrication technologies and thin film deposition on flexible Kapton substrates. As shown in the **Figure 3**, the

strain gauges will be allocated on a single foil w on each side of the finger and a common signals bus. The sensorized polymeric foil will be integrated by embedding it onto the finger's joints without compromising the bending capability.

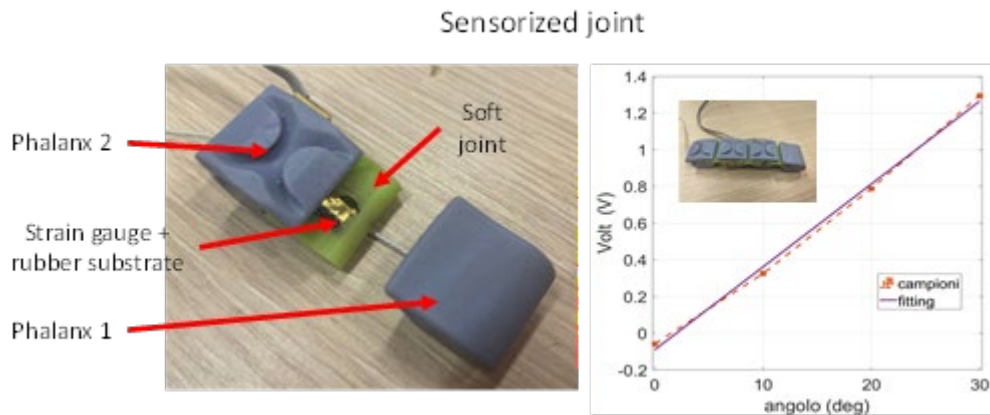


Figure 2 - Preliminary results with first prototypes.

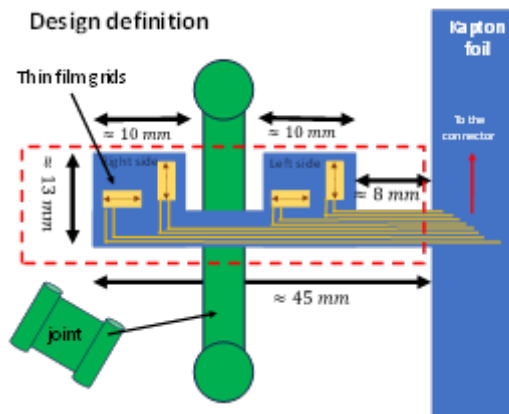


Figure 3 - Thin film sensory system with thin film technology - design definition.

The same thin film technology will be applied to the development of tactile sensors.

1.1.4 Human sensing for controlling the device

As far as the sensorization of the person wearing the soft robot is concerned, great advancement can come from the development of a tailored sensor body network, encompassing sensors (wearable) and embedded processing capability (edge computing). Moreover, regarding the development of sensor to monitor the person wearing the robot and to control the device movement, we started to investigate the possibility of using NIRS technology.

1.1.4.1 Wearable sensors and edge computing

State of the art

The history of Edge Computing has been shaped by the growing demand for bandwidth and the widespread use of connected devices, including IoT devices and wearables. This surge in connectivity has put significant strains on existing network infrastructures, leading to the identification of new challenges in data and resource management [9], [10]. To address these issues, new strategies and solutions were evaluated, and Edge Computing emerged as a crucial response to optimize real-time data processing and ensure efficient, low-latency connectivity in an increasingly interconnected world.

Edge Computing is an innovative technology that is revolutionizing data management in computing environments. This approach brings data processing closer to its source, rather than transferring it to central servers or remote clouds. In the realm of healthcare electronics, Edge Computing offers substantial benefits, significantly enhancing the efficiency and quality of medical care [11], [12]. It does so by reducing latency, which is the delay between data generation and processing, leading to a marked improvement in response times, which is of utmost importance in the medical field. Moreover, operational efficiency is greatly enhanced, with local data management optimizing resource utilization and healthcare infrastructure, thus improving data access and patient management. This innovative approach brings various advantages to healthcare electronics, such as faster response times in diagnoses and treatments, increased reliability and security of patient data, efficient management of the growing volume of healthcare data, cost savings associated with data transmission, and support for real-time services like remote patient monitoring and telemedicine.

Regarding wearable sensors, e-textile technologies are revolutionizing the world of smart clothing by enabling the seamless integration of sophisticated electronic components into fabrics. Among these components, MEMS accelerometers (Micro-Electro-Mechanical Systems) and integrated circuits play a prominent role in measuring various biomedical parameters, allowing for the precise monitoring of body movements, postures, and physical activity. These technologies not only facilitate personalized healthcare and sports performance monitoring but also offer the unique ability to assess and improve patients' posture during rehabilitation. Smart garments with integrated electronics can determine whether a patient is correctly performing exercises, making them invaluable tools for rehabilitation, thus promoting overall health and well-being. Additionally, they can measure vital signals such as ECG, respiration, skin temperature, and blood oxygen levels.

These technologies have been utilized for years in various fields, including space, exemplified by Astroskin—a vest enriched with multiple sensors capable of accurately recording a range of vital parameters for 48 hours [13]. In 2018, S. Uran and J. Geršak integrated a battery-powered printed device into the lower back of pants belts, employing accelerometers to monitor falls in individuals with dementia [14]. Moreover, Frances Cleary et al. in 2021 presented the design, development, and validation of an e-textile embroidered PLA smart garment. This intelligent garment facilitates on-body edge computing capabilities, reducing dependence on additional devices for computations. These innovations are made possible through the amalgamation of new materials in the e-textile sector, seamlessly blending with electronics and reshaping the landscape of healthcare monitoring, particularly in tracking the psychophysical state of patients.

Objective and activity

Expanding on this concept, we propose to investigate the feasibility of harmoniously integrating commercial sensors into textiles to create a proof of concept. Possible sensors for integration could include accelerometers for precise motion tracking and posture monitoring or thermometers for measuring temperature. This forward-thinking approach aims to demonstrate how existing sensors can seamlessly become part of smart fabrics, ushering in a new era of applications for wearable technology. This innovative proposition, which intends to integrate edge computing techniques with the sensors, seeks to broaden the range of applications for these cutting-edge technologies, transcending their traditional roles in military and space-related contexts, and introducing them into our daily lives. By integrating these advanced technologies into everyday clothing and accessories, it should be possible to enhance personal healthcare monitoring, sports performance optimization, and a myriad of other applications that will ultimately contribute to an improved quality of life. This is evidenced by the fact that the introduction of edge computing techniques adds a level of efficiency and timeliness to data processing. Data analysis can occur directly on the device (edge) rather than on a remote server, enabling faster responses and reducing the need to transfer large amounts of data.

1.1.4.2 Muscle activity monitoring through NIRS Technology

NIRS is a valuable technology to monitor muscle activity [11]. It offers a non-invasive and adaptable approach for analyzing physiological changes unfolding within muscles during a spectrum of activities.

NIRS offers the ability to measure the concentration of two key players: oxygenated hemoglobin (HbO₂) and deoxygenated hemoglobin (Hb) within muscle tissue and, consequently the total blood volume [11]. like EMG and ultrasound sensors. Muscle contraction invariably reshuffles the blood volume within the tissue. This, in turn, produces observable variations in the near-infrared signals [12]. Therefore, NIRS can be advantageously combined with other sensors to control prosthesis movement.

Objective and activity

In this research project, our objective is to create and implement NIRS sensors within prosthesis control systems, enhancing overall performance.

The current activity is focused on the literature analysis, concentrating our efforts on understanding both the limitations and advantages of NIRS technology, with its non-contact measurement capability being a significant advantage. Furthermore, we are exploring how an NIRS sensor can be seamlessly integrated into a complex sensing system alongside other types of sensors, like EMG and ultrasound sensors.

Subsequently, we are working on defining optical geometries. The choice of optical geometry is a critical aspect of sensor design as it directly impacts the accuracy and reliability of measurements.

1.1.5 Interaction with the environment

Finally, with the aim of having a seamless experience and a safe interaction with the environment, we also considered the development of a heterogeneous sensorimotor representation of the surrounding space.

State of the art

In robotics visual perception of the end-effector has been traditionally neglected or simplified using custom markers. This is acceptable in industrial setting where the environment is controlled and the focus is on the problem of positioning the end-effector. In assistive and collaborative (as well as wearable) systems for human-robot interaction for industrial and domestic applications to increase inclusion and autonomous living of persons with special needs, disabilities or impairments, the problem becomes more complex, as it is important to make sure that any part of the robot does not collide with obstacles and humans [18].

A future in which robots will be increasingly engaged in symbiotic interactions with human operators makes it urgent developing embodied systems which “learn” representations for and from action and interaction. Actually, in natural systems the sense of space should be understood as an emergent property from dynamic integration of heterogeneous information collected by distributed embodied sensors.

This subproject in part builds upon the scientific and technical achievements of the group on robot skin technologies and related skin-based control methods, and their applications to develop new generations of robots capable of interacting safely in close and complex way with objects and humans. One of the key aspects that emerged has been the need to map the 3D distribution of the tactile sensors placed all over the robot body onto a planar 2D manifold where tactile data can be managed (including processing) without the explicit need to consider the actual robot shape. Yet, this “static” somatosensory representation, which can be considered analogous to the somatotopic map representing the skin mechanoreceptors on the brain cortex, is not sufficient to provide a complete robot body 3D representation useful for planning and control robot’s motions.

Objective and activities

The main goal of this subproject is to develop models for the representation of the robot body based on the integration of different sensory modalities (multi-sensory integration) like touch, vision, proximity sensor, and proprioception. This will eventually endow robot with a complete body-scheme in which several parts of the limbs (and not only a single point or sketched representation) are represented. It has been demonstrated that such a representation exists in the primate brain. In particular, experiments have demonstrated the existence of neurons responding to visual and tactile stimulation of the arm and the face [19], [20]. The sensory response of these neurons presents a tactile receptive field (RF) with an aligned visual RF that extends in 3D space around the tactile RF (typically an object moving towards that part of the body underlying the tactile RF elicits a “visual” response of the neuron). Remarkably, keeping visual and tactile RF aligned requires that proprioception is correctly taken into account. In engineering terms, this means that the brain uses the signals encoding the position of the arm and the head to compute the appropriate coordinate transformation that projects the tactile/proximity RF attached for example to a part of the arm, onto the corresponding location on the image plane. The result would be a pre-attentive awareness of the space immediately surrounding the body while interacting with the environment. Such an awareness will derive from information actively captured by vision, and embedded proxy-tactile sensors, possibly integrated with acoustic sensors. Our interest is in the final representation, but also in the process that let the robot autonomously build this representation. A similar approach has been taken by Fuke [21], although in simulation.

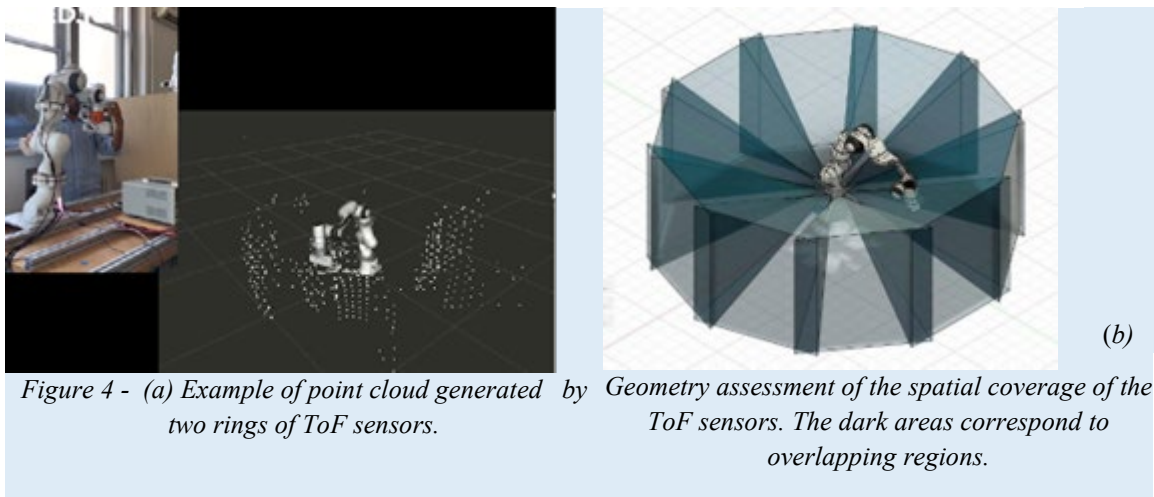
Two activities will be specifically pursued:

Activity 1: Heterogeneous space perception anchored to the robot body. Develop multimodal peripersonal space perception by remapping the information gained by the real sensors (namely, skin-like tactile sensors, proximity sensors and cameras actively moved by the body) with respect to the body surface.

Activity 2: Reactive on-line sensorimotor control. Develop multimodal control modules capable of handling unexpected, altered goals e.g., in reaching/grasping tasks. Modules will eventually rely on multimodal perceptual engines developed in Activity 1.

Achievements

A preliminary testbed for proximity sensing. A set of Time-of-Flight (ToF) devices has been integrated onto a robot. Each ToF acquires an 8x8 depth image which contributes to a space-time varying sparse point cloud around the robot. The work has focused on the optimization of the displacement of the sensors on the robot body in terms of number and system design complexity. The present solution is based on sensor rings strategically placed to ensure partial overlapping of the volume sensed by each ToF. The sensing architecture is currently under development; the design strategy targets two major engineering goals: 1) to ensure electromechanical integration on the target robot; 2) to ensure low latency data acquisition for future ToF based feedback robot control.



A visual-based distributed representation of 3D space in egocentric (i.e., body-centered) coordinates: By properly modulating the response of a population of binocular disparity detectors [22], [23] through gain fields that depend on the current gaze direction (azimuth and elevation) we demonstrated it is possible to obtain a set of "depth sensors" independent of the relative position of the stereo cameras.

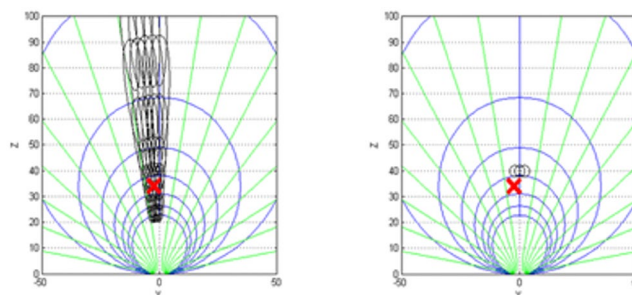


Figure 5 - Simulation results of the emergence of gaze-independent 3D detectors. (Left) Ellipses represent the regions of sensitivity in the 3D space for a set of detectors. In principle, a population of detectors would properly tile the 3D peripersonal space around the robot's body. (Right) Regions of selectivity of the resulting gaze-independent 3D detectors. In both figures the cyclopean eye is located in (0,0) and the red square represents the contingent binocular fixation point. Blue circles represent iso-vergence points, whereas green lines represent iso-vergence points.

1.2 CATE (COMPLIANT ACTUATION FOR WEARABLE ROBOTS)

1.2.1 Research team

The research team involved in this project encompasses 4 research units, namely the University of Genova (UNIGE), University Campus BioMedico (UCBM), University of Naples (UNINA), Institute of Electronics and Information & Telecommunication Engineering of the National Research Council of Turin (CNR-IEIIT).

The composition of the research team is detailed in the following **Table 2**.

Table 2 - Research team.

UNIGE	Giovanni Berselli, Mario Baggetta, Greta Vazzoler, Seyyed Masoud Kargar
UCBM	Loredana Zollo, Nevio Luigi Tagliamonte, Fabrizio Taffoni
UNINA	Fanny Ficuciello, Marco Caianiello, Sajjad Hussain
CNR-IEIIT	Fabrizio Dabbene, Martina Mammarella

1.2.2 Introduction

Wearable robotics have been significantly advanced during the last decades, resulting in a wide variety of devices adopted in therapy, assistance and occupational domains. The mechatronic design of these robots is a crucial aspect that affects the efficiency and effectiveness of their interaction with the user. Most developments have pointed towards compliant actuation and structures, due to their potential in terms of adaptability, safety, efficiency, and comfort [19], [23].

Compliant actuators have been extensively explored in literature and the most adopted solutions include Series Elastic Actuators (SEAs) and Variable Stiffness Actuators (VSAs). SEAs are characterized by the presence of an elastic element with fixed stiffness placed in series to geared motors. This strategy has shown improved performance in terms of human-robot interaction, safety, energy efficiency, shock tolerance and back-drivability, when compared to stiff actuators, and also reduced cost due to the use of angular sensors instead of expensive torque sensors [24], [25]. VSAs are a variation of SEAs, in which compliance can be mechanically modulated to change the actuator output characteristics thus adapting to environmental changes, and possibly reducing energy expenditure.

The mechatronic design of compliant actuators is still an open challenge and requires multiple trade-offs between performance (e.g. control bandwidth) and wearability (e.g. reduced weight and encumbrance). The inclusion of intrinsic elasticity, not only in terms of stiffness selection, but especially in terms of the adopted mechanical solution, poses several difficulties. This aspect together with the need to include sensing elements, transmissions and additional supporting components (e.g. bearings) very often lead to significant actuators complexity. From the mechanical point of view the design of elastic elements requires an arduous trade-off between the need of compliance (soft materials are beneficial but they cause drawbacks such as non-linearities, limited controllability and resistance) and robustness (metallic parts are beneficial but they cause drawbacks such as increased weight and limited compliance). How to merge the benefits of rigid and soft elements in compact designs for the actuation of wearable robots is still a hot research question [26], [27].

Objectives

The project aims to explore new approaches for the smart distribution of soft and rigid elements in the development of compact compliant actuators to be applied in wearable robots. In particular, it adopts new solutions for the merging of more traditional rigid components, such as gears, bearings and electric motors, with novel designs of soft elements, based on the smart distribution of materials or on the inclusion of flexible mechanisms or on custom compliant elements. Also, the seamless integration of sensors within the mechanical design is targeted to avoid a net disjunction of structural, actuation and sensing functions. Special attention is given to harmonize the distribution of all the components to achieve compact design in favour of lightness and wearability. In this sense, the project aims not at merely connect a series of functionally separated components but rather at trying to blend them and their functions by means hybrid multi-function solutions: compliant bearings (bearing elements with integrated compliance), structural sensing (structural elements with integrated sensing capability), differential transmissions (reduction gears with serial connection capability) and similar approaches will be explored.

A central aspect of the project is the development of compliant elements. In this regards CATE is analyzing different possibilities, e.g. taking into account in a broad way the potentialities of several solutions:

- i. components made of rigid materials with structural/geometrical features introducing compliance
- ii. intrinsically soft materials and working principles typically used in soft robotics
- iii. cable-driven solutions often adopted in soft exosuits.

Pros and cons of different or mixed approaches are currently under analysis.

In summary, the project proposes at least on compliant actuator for wearable robots developed on a smart allocation of soft and rigid elements.

1.2.3 Research activities and achievements

The following activities are being carried out:

- **Activity #1:** Identification of design requirements, definition of technical specifications, analysis of state-of-the-art actuators and drafting of promising solutions and novelties.
- **Activity #2:** Selection of basic commercial elements. Design of different solutions for actuator components in hybrid multi-function configuration with special focus on compliant elements and smart blend of functions, rigid-soft distribution and sensing. Preliminary proof-of-concept prototyping. Design of required testbed for subsequent performance testing.
- **Activity #3:** Advanced prototyping (mechanics, motor, sensing and preliminary electronics), implementation of basic control features, preliminary testing and comparison of different solutions. Iterative and progressive design refinement of a selected solution.
- **Activity #4:** Final electronics integration and advanced torque/impedance control implementation in the selected solution.
- **Activity #5:** Testing, control optimization/refinement and performance characterization of the final prototype.

1.2.4 Analysis of the state of the art on compliant components for rotary SEAs

Wearable robots, operating in close contact with humans, e.g. for industrial, rehabilitation and assistive applications, require actuators capable of accurately and safely modulating the delivered torques at the human joints level, to stably and robustly regulate human-robot dynamic interaction. Introducing compliance in traditional geared and position-controlled actuators, or more in general in the robotic structure, aims at satisfying this requirement. Several actuation solutions have been proposed in the literature and, as mentioned above, VSAs and SEAs are the most widely adopted type of actuators, for example in lower limb exoskeletons [28]. In most cases actuators are rotary since they can be more easily aligned with human joints to be supported.

SEA architecture is a simple and effective solution, which basically consists of a gear-motor in series to a spring connected to the load [29], [30]. This solution allows to decouple the actuator output from motor inertia and other nonlinearities, with benefits in terms of torque control fidelity. Additionally, the delivered torque can be simply estimated by measuring the deflection of the elastic element and can be used to implement torque control, as depicted in the simplified scheme of **Figure 6**. Indeed, the spring deflection $\Delta\theta$ provides an estimate of the torque delivered by the actuator τ_l . This measure is used as the feedback signal for the torque controller, which at a lower level becomes a simpler position or velocity controller.

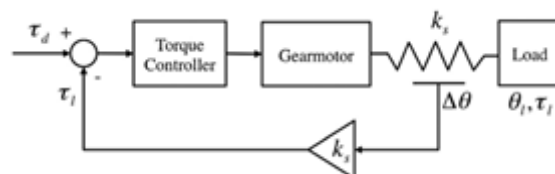


Figure 6 Simplified torque control scheme for a rotary SEA adapted from [31]. τ_d represents the desired torque, k_s the spring stiffness, $\Delta\theta$ the spring deflection, τ_l the output torque and θ_l the output angle.

The intrinsic compliance of SEAs guarantees low impedance across the whole frequency spectrum (for external perturbations at frequencies above the controllable bandwidth, the impedance reduces to the stiffness of the spring, thus avoiding unsafe behaviors due to sensors failure and/or control bandwidth limitation). Moreover, a higher compliance in the torque control loop allows increasing the control gains within fixed stability margins [30]. This results in a reduction of the effects of internal stiction and other transmission nonlinearities (friction and backlash) and in an improvement of the torque tracking. In [32], it has also been proved that a proper selection of spring stiffness, according to a specific application, can lead to an energetic optimization of the system due to energy storage and release. Recently, an example of an energy storage device combined with a rotary SEA has been presented [33], in which two springs are exploited. An application of this solution could be exoskeletons for lumbar support or for locomotion, in which elastic potential energy is stored and then released, contributing to energy efficiency.

The major drawback introduced by the elastic element of SEAs is the reduction of the actuator bandwidth [34]: a higher compliance of the actuator reduces the bandwidth of the torque control. Other drawbacks include the increase in the production/maintenance costs, complexity and failure risk, since including elastic elements entails additional components (bearings, sensors, connection parts, etc.) [35]. These drawbacks can vary depending on the specific field of application but in most cases the benefits outweigh disadvantages, especially when the benefits are safety, precision and adaptability which are inherent in the use of SEAs. Furthermore, some drawbacks can be curbed wisely choosing the kind of elastic component to be included.

The selection of the elastic component type and stiffness remains a major open challenge for SEA designs [28]. Indeed, the stiffness of a series elastic element must be a trade-off between performance, adaptability and safety. From the control point of view, higher stiffness increases the control bandwidth [36]. However, this can hinder the intrinsic compliance/adaptability. From the safety point of view, compliance can adsorb unexpected impacts [31]. Nevertheless, energy stored in a spring can be even suddenly released during impacts or device misuse thus generating unexpected and unsafe reactions [37]. From a mechanical perspective, the main challenge is the achievement of low stiffness while guaranteeing an adequate robustness with respect to high torques to be delivered by the actuators. Moreover, dimensions and weight must be reduced as much as possible, especially for wearable robotics applications. From a sensorization viewpoint, high stiffness requires higher resolution for deflection sensors, given a target resolution in the torque measurement. Furthermore, to avoid nonlinear control schemes and to allow homogeneous regulation capability over the whole range of deliverable torques, a linear torque versus angle characteristic is desirable. Indeed, nonlinear relationships would imply an increased sensitivity to motor positioning inaccuracies, thus possibly implying regulation errors in case of large torques.

This compliant/rigid dichotomy makes it clearly difficult to select a proper stiffness value [28]. Multiple selection criteria have been used [38]. One of the most common consists in setting the spring stiffness as the slope of a desired torque-angle characteristic [39]. Another common principle is based on maximizing the energy stored and released throughout a working cycle [40], [41]. Finally, the selection of the optimal spring stiffness should involve not only a theoretical analysis but also an experimental validation for the specific application [39], [42], [43].

A significant amount of research in SEA development has been focused on designing custom components suitable to match the specific requirements of a given application. Adapting the information reported in [28], [31], [33], [44], four categories of elastic components for rotary SEAs can be identified, depending on the solutions adopted to implement the desired output torsion stiffness, as described below.

Arrangements of linear compression springs

This category comprises compliant components adopting linear compression springs arranged in such a way that a centering elastic torque is produced when the joint shaft is rotated [45], [46]. Some examples are reported in **Figure 7**. A system with a three-spoke output component, a circular input pulley and six linear springs was presented in [47] (**Figure 7 a**). A similar approach, where six linear springs are used, is described in [48] (**Figure 7 b**). In [46], [49], four springs have been used in a similar way. In the SEA described in [45], the torsion elastic behavior is demanded to the agonistic-antagonistic configuration of two linear compression springs connected to the actuator pulley by a cable (**Figure 7 c**). A similar approach is pursued in [50] (**Figure 7d**).

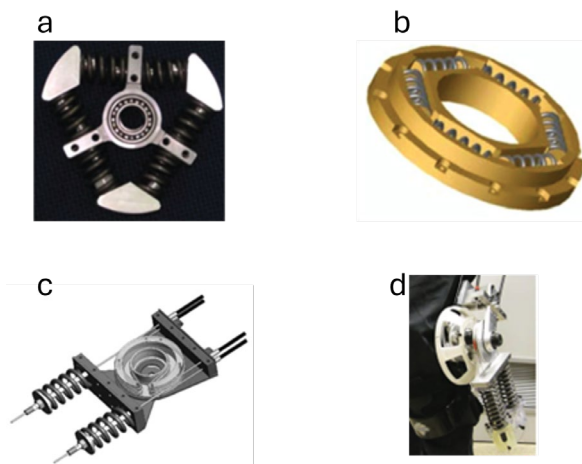


Figure 7 - Examples of compliant components based on arrangements of linear compression springs. [47](a), [48](b), [45](c), [50](d).

Helical torsion springs

This category comprises compliant components employing simple helical torsion springs embedded in the transmission train or on the load side [51]. This solution is quite simple, since helical springs are easily available on the market, but does not allow to obtain a specifically desired stiffness value. Some examples are reported in **Figure 8**. In [51] (Figure 3c) the spring is mounted between the worm gear and the output gears. However, some loss of force transfer fidelity occurs due to the nonlinearities associated to output gears. This drawback can be circumvented by directly placing the spring between the gearmotor and the load.

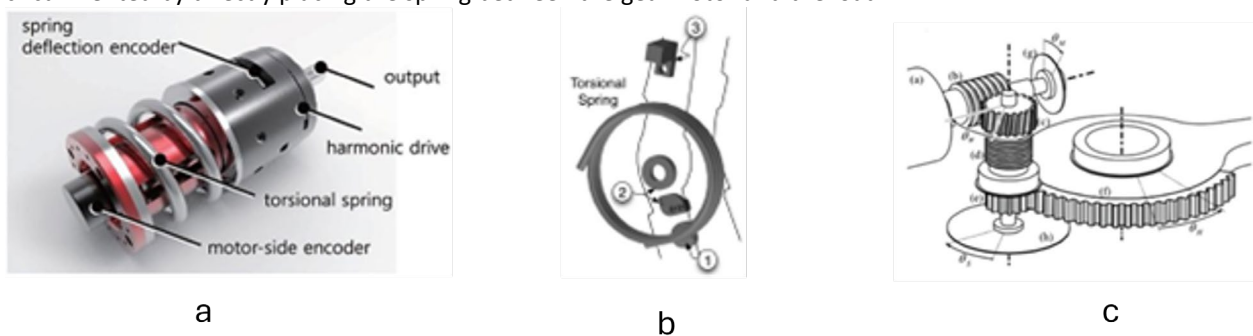


Figure 8 - Examples of compliant components based on helical torsion springs. [52] (a), [53] (b), [51] (c).

Spiral torsion springs

This category is similar to the previous one. It comprises compliant components employing springs designs based on the traditional mathematical Archimedes spiral. The springs included in the systems belonging to this category can be either commercial or custom. In the second case a design based on the Finite Element Method (FEM) is carried out so that parameters are varied to obtain a desired torsion stiffness. Examples reported in **Figure 9** describe custom spring designs, implemented for a biped robot (a) or wearable robots (b, c).

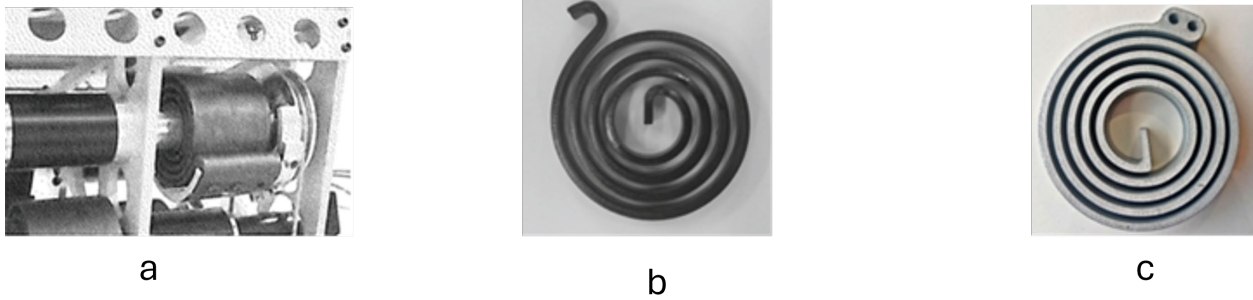


Figure 9 - Examples of compliant components based on spiral torsion springs. [54] (a), [55] (b), [56] (c).

Disc-shaped structural torsion springs

This category comprises compliant components based on a monolithic disc-shaped design. Many works have been recently dedicated to this kind of designs, as overviewed in [33], [28]. These solutions are custom-designed and are developed in a wide variety of manufacturing materials, such as maraging steel (martensitic steel with aging treatment) or high-grade titanium. The geometry is usually defined through an iterative FEM-based simulation-process, carefully carried out to make sure that the elastic component is able to withstand the expected torque and deformation. FEM leads to the optimization of some dimensional parameters that are left free, keeping fixed the dimensions constrained by the footprint and the connection with the actuation unit and the load (i.e. the inner and outer diameter of the compliant element). This optimization is done by considering stress reduction and desired torsional stiffness, as aforementioned goals, but also taking into account manufacturability, material, and bulkiness [57]. Nonetheless, results from simulations often do not match experimental results, for instance with respect to the actual stiffness [42], [58], thus requiring a dedicated and accurate experimental characterization/calibration of the elastic components based on tests after fabrication. Many examples are reported in **Figure 10**, mainly adapted from [33]. Among all the possible shapes that have been explored in literature, it is worth mentioning the custom-made double spiral spring presented in [51] (**Figure 10 a**), based on the previous design in [59] (**Figure 10 b**). This double spiral design is an evolution of the solutions based on spiral torsion springs presented above, since it cancels out undesired radial forces acting on the spring center when the spring is deformed by a torque.

It is of interest to highlight that, disc-shaped structural torsion springs for SEAs are in most cases manufactured with materials with a high yield strain and Young Module to deal with the necessity of the component to work in its linear elastic range, avoiding nonlinearities in the torque-angle behavior and in delivered torque (which could demand a more complex control). Indeed, very spread materials for this application are alloy steels. Some open design challenges, hence, could include the use of softer materials and possibly the use of smart solutions with intrinsic structural sensing.

1.2.4.1 Computer-aided tools for optimal design of compliant elements

As previously recalled, VSA and SEA requires the inclusion of compliant transmissions for their functioning. From a functional standpoint, such requirement translates into the necessity to design non-linear spring elements whose behaviour shall be tailored to the application at hand. Ideally, these non-linear springs shall be characterized by a pre-determined behaviour in terms of force/torque displacement curves (i.e. compliance), as well as predictable time-dependent properties (i.e. damping) so as to be effectively employed in mechatronic devices requiring compliance and impedance regulation. Within this scenario, one of the CATE activity is to produce computer-aided design tools for the optimal design of such elements, with user-friendliness in mind. At the current state, the design tool framework leverages on the connection of 1) a parametric CAD; 2) an flexible multi-body dynamic (MFDB) solver; 3) an external optimizer (implementing meta-modelling optimization routines). In particular, although specific tools may vary, we are leveraging on the capabilities of CREO parametric as CAD, of Recurdyn MFBD connected via Matlab code.

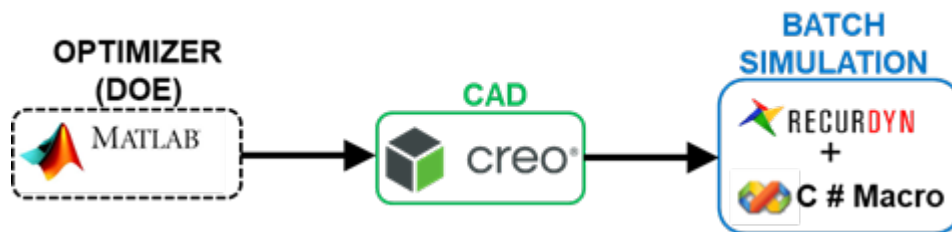


Figure 11 - Computer-Aided framework for optimal design of compliant elements.

Such framework has been employed in the optimal design of a VSA to be used as elbow joint in e.g. upper-limb prosthetic devices. **Figure 12** and **Figure 13** Report the virtual and physical prototypes of such device along with a schematic of the employed non-linear spring shape.

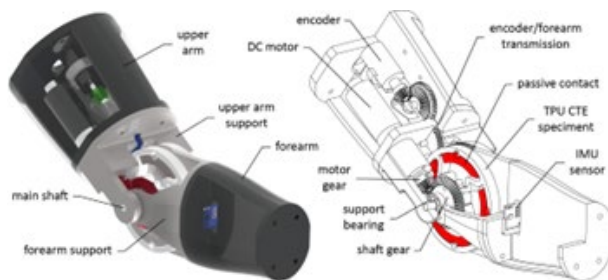


Figure 12 - Variable-stiffness elbow joint. CAD model.



Figure 13 - Physical Prototype.

1.3 TEST DEM (TAILORED ENERGY STORAGE DESIGN, EXPERIMENTATION AND MODELLING)

1.3.1 Research team

The research team involved in this project is composed of 7 research units, with different roles.

The composition of the research team is detailed in the following **Table 3**.

Table 3 – Research team.

CNR-STEMS	<i>Research Technologist:</i> Clemente Capasso <i>Researcher:</i> Luigi Sequino <i>Research Managers:</i> Bianca Maria Vaglieco, Ottorino Veneri <i>Technicians:</i> Antonio Rossi, Carlo Rossi, Bruno Sgammato
-----------	--

1.3.2 Introduction

In recent years, robotic and mechatronic devices have been significantly developed as valuable biomedical tools. In fact, nowadays, people can monitor their daily health, using state-of-the-art biomedical systems such as skin-patchable and implantable devices. These devices are in continuous evolution and, supported by new IoT and ICT technologies, are able to provide communication services with external systems and databases for real-time tracking, diagnosis, and treatment. It is clear that, for self-powered systems, in order to achieve such crucial services, the right amount of electric power must be continuously and reliably supplied. As a matter of fact, a small part of this power can be obtained by using energy coming from biomechanical and renewable sources, which for their intrinsic nature are generally considered as unpredictable sources. Therefore, reliability requirements must be guaranteed through the integration of high-performance Energy Storage Systems (ESSs). At the same time, with increasing power demand, ESSs are also becoming a key technology for optimization of the overall system energy efficiency. Indeed, one of the most recent techniques to reduce the energy demand of these systems is the use of energy recovery devices. The main idea behind these devices is to harvest energy during braking phases, by storing it in proper storage systems, and to provide it to the system when required [71].

Starting from the above context, preliminary activities carried out in the first part of the TEST-DEM sub-project consist of critical analysis and comparison of storage solutions for robotic applications, with a particular focus on available storage technologies with the related possible optimization solutions. Starting from this analysis, specific devices have been identified on the market for experimental tests on storage modules to be carried out in the Center of Excellence for Sustainable Energy Sources. Finally, case studies reported in the scientific literature have been investigated in order to evaluate examples of energy/power requirements for specific bio-robotic applications

1.3.3 Critical analysis of available storage devices and evaluation of possible solutions for cooling and design optimization

1.3.3.1 Main battery technologies for bio-robotic applications

As mentioned above, ESSs technologies play a relevant role in bio-robotic applications, both for supplying stand-alone devices and for optimizing system energy efficiency.

In particular, electrochemical batteries, based on different materials, represent the main energy sources for stand-alone mobile robot applications. Therefore, depending on the specific application, different elements need to be considered for the proper choice and sizing of storage technology to be used.

Focusing on the available storage technologies, lead-acid batteries are characterized by one of the lowest costs (per Wh) available on the market. This factor, together with other advantages in terms of availability of materials and reliability, has supported, in the past years, the wide diffusion of this technology, especially for stationary applications. Nowadays, a great part of the available lead acid storage modules is based on VRLA (Valve Regulated

Lead Acid) technologies, which are characterized by lower maintenance costs in comparison with the old VLA (Vented Lead Acid) modules. Despite the above advantages, the specific energy provided by lead acid technology is very low (35–40 Wh/kg) with power density values up to 150 W/kg [72]. In addition, these technologies reach the end of life very early, after about 800 complete charging/discharging cycles. For this reason, the use of lead acid batteries is generally limited to a few specific applications where cost requirements have primary importance in comparison with space and weight requirements. An example of these applications can be represented by the autonomous mobile robot *HOSPI*, produced by Panasonic for medicines delivery within hospitals. The robot is characterized by an overall weight of 170 kg, comprehensive of lead-acid batteries, with an autonomy of about 9 hours. In this case, the typical operative mission of the robot is well-known, and batteries can be slowly charged during a resting period of about 4.5 h [73].

In the case of either mobile or wearable robot applications, space and weight may become key requirements to be satisfied. For these applications, lithium batteries represent one of the most promising electrochemical storage technologies. The reasons behind the increasing interest in lithium-based storage technologies can be mainly found in their high energy and power density, which have boosted their use for powering both portable electronic devices and high-power applications (e.g. electric/hybrid vehicles).

Lithium cells are produced in different shapes, which can be used for obtaining custom battery pack shapes and layouts. In particular, *cylindrical cells* are very similar, in shape, to the commercial batteries available for TV remote controllers. The most common format is 18650 (diameter = 18 mm, height = 650mm), 21700, and 26650 even though customized solutions can be found on the market on the basis of manufacturer choices. The advantages of using cylindrical lithium cells mainly rely on the resistant case and the possibility of using the same shape for different chemistry. *Pouch cells*, so called because of their envelope shape, are characterized by the main advantage of increasing the overall specific energy thanks to the thickness of their case. On the other hand, for the same reason they have less protection against external collisions and may be subject to swelling during their operative life. Prismatic cells have a solid case normally made of plastic or metal (aluminum) and generally provide screw poles for easy series/parallel connections. The main advantages are related to the case, which guarantees high resistance toward mechanical stress, and the possibility of reaching high energy values for each single cell, reducing the number of required parallel connections.

A picture of the above cell shapes, with the related characteristics, is reported in **Figure 14** [74].

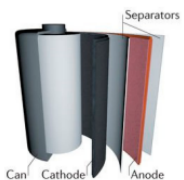
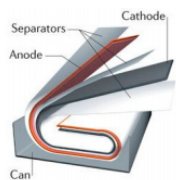
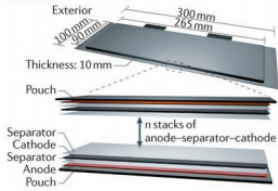
Shape	Cylindrical	Prismatic	Pouch
Diagram			
Electrode Arrangement	Wound	Wound	Stacked
Mechanical Strength	++	+	-
Heat Management	-	+	+
Specific Energy	+	+	++
Energy Density	+	++	+

Figure 14 - Main lithium cell shapes.

In the following main lithium technologies, to be used in robotic applications are reported [75].

Lithium Cobalt Oxide (LiCoO₂): This technology was firstly developed in the early 90s by Sony and has been widely used for portable electronic devices thanks to its high performance in terms of energy density and durability. On the other hand, these batteries are characterized by poor thermal stability and required constant monitoring during their operations. In addition, their cost and diffusion are strongly affected by the reduced availability of Cobalt.

LiFePO₄ (LFP): One of the phosphates most commonly used is the LiFePO₄ technology, based on olivine crystal structure, which has shown promising characteristics when supplying road electric and hybrid vehicles. The main advantages of LiFePO₄ batteries are based on the low cost, long cycle life and high availability of Fe, high thermal stability and safety properties, due to the strength of the covalent Fe–P–O bond with respect to Co–O bond, which reduces the risk of oxygen release [76]. Their energy density is lower than LiCoO₂ cathode, but their main limitation is represented by a low electrical conductivity, which is usually faced either by reducing the particle size, or coating/doping the LiFePO₄ particles with conductive additives [77]. Nowadays LiFePO₄ has completely replaced lead acid batteries as one of the most commonly used technology, for supplying autonomous mobile robots in the bio-medical sector. In particular, examples of applications for these storage technologies are represented by the indoor delivery and disinfection robots produced by different companies (e.g. IAM Robotics, Reeman Robots, etc..) and used within hospitals for medicine transportation [78],[79].

Lithium Nickel Manganese Cobalt Oxide (Li(NixMnyCo1-x-y)O2): Lithium Nickel Manganese Cobalt Oxide (NMC) electrodes are generally used for high specific energy or power density. The main innovation of this technology is based on the combination of nickel and manganese: nickel presents high specific energy but poor stability; manganese has the benefit of forming a spinel structure to achieve low internal resistance but with low specific energy. The mix of the two metals (nickel and manganese) varies by manufacturer since using nickel-rich electrodes can increase energy density, while reduction in cobalt is also helpful since it lowers costs. The combination of nickel and manganese has made NMC technology the most successful Li-ion system for EV powertrains. On the other hand, thanks to their high specific energy and excellent thermal characteristics, the use of these systems for robotic applications is increasing more and more, especially in cases of long-operative missions where energy demand dominates the selection process.

Lithium-titanate battery (Li₄Ti₅O₁₂): This technology, also known in the battery industry as LTO, is a modified lithium-ion battery that uses lithium-titanate nanocrystals on the surface of its anode instead of carbon graphite. Lithium titanate is a promising anode material for specific applications that require high rate capability and long cycle life. LTO is interesting as it offers advantages in terms of power and chemical stability, although LTO based batteries have a rated voltage of 2.4 V/cell, which is lower than LiCoO₂ and LFP. On the other hand, the lower operating voltage is balanced by significant advantages in terms of safety. Further, these batteries have fast charging rate, in fact they can be safely charged at rates even higher than 10 C, which means charging times lower than 10 minutes for this kind of battery. The LTO based batteries have also the characteristic of an operating temperature range wider than other lithium battery technologies, in particular, they have excellent low-temperature discharge characteristics with an actual capacity of 80% at 243K. Moreover, their life span and power density are not lower than other lithium batteries, and the recharge efficiency can be even higher than 98%. On the other hand, the energy density of 65 Wh/kg for the LTO based batteries is higher than lead acid and NiCad batteries, but it is still lower than other lithium ion batteries [80]. The advantages in terms of thermal stability, durability and charging times of LTO technologies have encouraged their use in medical environment with particular reference to medical electronics [81], and portable Medical Equipment [82].

LiNi_{1-x-y}Al_xCo_yO₂, (NCA): NCA materials are one of the most promising cathode materials for high power applications. The term NCA refers to a lithiated ternary metal oxide consisting of Ni, Co and Al, in various stoichiometric ratios. Despite many attractive electrochemical properties of the NCA technologies, various aspects, mainly related to poor thermal/cycle stability and low electronic conductivity, are still considered problematic. The thermal stability of NCA may be an issue for heavy-duty, high-power demands. In addition, this technology suffers from relevant capacity fading at elevated temperatures (40–70 °C). Therefore, in most of the cases, LFP technology is preferred [83].

1.3.3.2 Advanced cooling solutions for battery performance improvement

The type of battery technology to identify for medical robotic applications is crucial as previously seen. A fundamental support to the safe and efficient functioning of the battery is provided by the conditioning system. In general, the batteries have a limited temperature range where the best performances are granted. Therefore, in case of cold environment they must be warmed as well as for hot cases they must be cooled. For medical robotics

applications, it is assumed that the system is placed in a comfortable environment and then the main issue may be related to the cell internal heat generation. For this reason, the study of cooling systems is considered of main importance.

In this phase of the project, the research activities focused on the investigation through literature analysis and experimentation of different cooling systems. The main investigated solutions consist in: the application of high conductivity layers to the cells to enhance the natural convection; the realization of fins with a non-conventional geometry using metal foams for the heat dissipation in natural convection as well; liquid cooling systems in forced convection conditions using 3d printed plastic channel plates.

The first innovative system for the heat dissipation of li-ion cells consists in the application of coatings of different materials [84]. A flat cell has been used for the tests to evaluate also the bi-dimensional temperature distribution across the surface. The study was first conducted on an uncoated battery that serves as a reference and subsequently using coatings of a carbon fiber-reinforced polymer (CFRP) composite and a coating of graphene nanoplatelets, applied to the carbon-fiber polymer. As prototype components, their thermal characteristics were unknown and then tests were performed on purpose to evaluate the thermal conductivity (reported in **Table 4**). Also, the battery conductivity across the transverse profile were evaluated with the same procedure. The coatings were applied to the rear side of the battery using a thin layer of silicone thermal grease with a thermal conductivity of 1.4 W/mK, close to that of the battery [85]. **Figure 15** top shows some photographs of the uncoated and coated cell with the carbon and the graphene layers.

Table 4 - Coatings specifications.

Coatings	Carbon	Graphene
Thickness [mm]	1.5	1.5
Conductivity [W/mK]	0.67 ± 0.13	0.86 ± 0.17
Battery conductivity is measured across the transverse profile = 1.1 ± 0.22 W/mK		

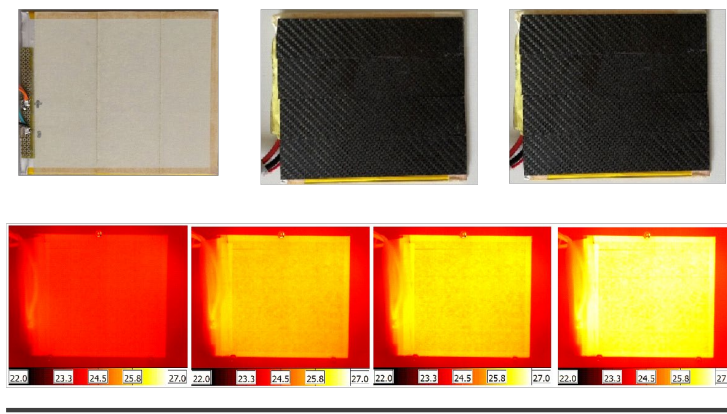


Figure 15 - Visible images of the flat cells w/ and w/o coating and infrared images of the no coating case during discharge.

In the bottom of **Figure 15** a collection of images recorded by the thermal camera during the test of discharge shows that the cell temperature slowly increases keeping homogeneous across the cell surface. The images refer only to the uncoated battery and have been reported to give an overview of the phenomenon. A mathematical procedure is performed on the images at each time step to derive the surface averaged temperature values. The results are plotted in **Figure 16** versus time. The cell heating and subsequent cooling follow an exponential behavior as described by the Newton's cooling law. The final temperature after the heating phase is higher for the uncoated cell.

The one with the graphene coating, which has the highest conductivity, reaches the lowest temperature. Whilst the temperature values during the cooling phase overlap.

This preliminary analysis shows that higher is the thermal conductivity of the applied coating, lower is the maximum cell temperature [86]. For intense working conditions or prolonged operation time, the observed differences can be significant. In particular, for wearable applications, where the component is very close to the user skin, a value of even just a couple of Celsius degrees higher than the body temperature can be detrimental for the comfort.

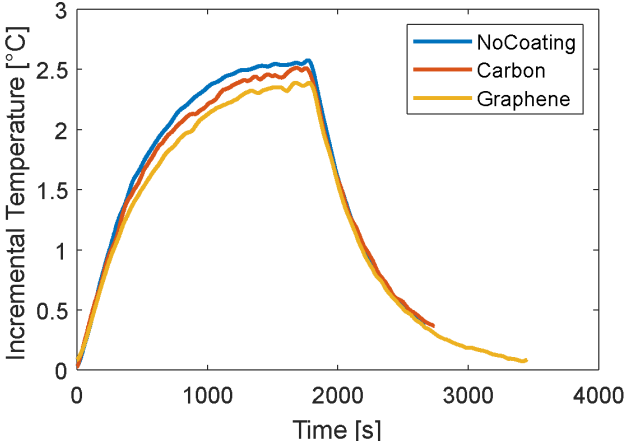


Figure 16 - Increment of temperature during the test of discharge for the coated and uncoated flat cells.

Concerning the second investigated solution, a metal foam-based frame was realized and tested with cylindrical cells. Metal foams are material with a characteristic geometry which provides them an “effective density” lower than their “apparent density”. The first is the ratio between the body mass and the metal volume. While for the second, the body mass is divided to the volume occupied by the component. The presence of holes, channels, and bubbles in the metal foam structure, strongly reduces its apparent density. In view of medical robotic applications, the metal foam-based frame has the advantage of high mechanical performance as it can be used both for the support of the cells and the heat dissipation, thanks to its good thermal properties. The metal foam-based frame used in this analysis is based on an aluminum alloy and presents a high degree of “open-ness”. A layout with two 18650 cylindrical cells connected in series are adopted as example of a small battery pack. Two configurations are tested to perform a comparative analysis as shown in **Figure 17**: A) cells with plastic support (reference case); B) cells mounted on the metal foam-based frame.

Figure 18 reports a collection of images of the two configurations at the start of the test (1s), at the end of the heating (4500s), and at the end of the cool-down (5050s). A slight difference can be appreciated between the two configurations during the heating phase but it is not immediately quantifiable from the images. Moreover, also the temperature variation of the fins systems of metal foams can be followed.

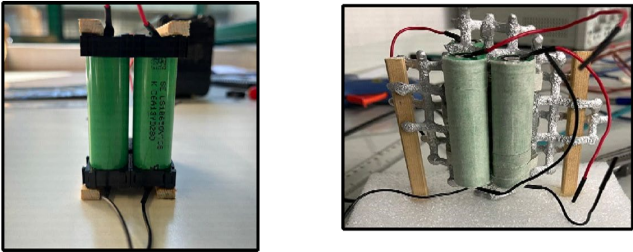


Figure 17 - Tested configurations of the 18650 cylindrical cells for the analysis of the metal foam-based frame performances.

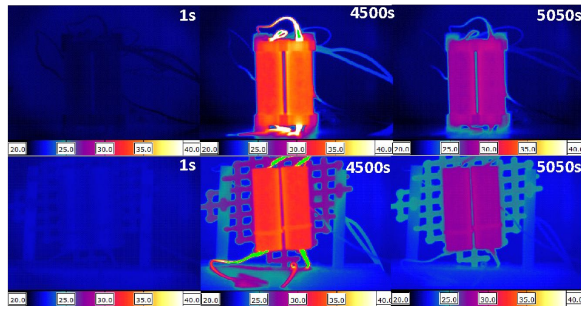


Figure 18 -infrared images of the two configurations at the start of the test (1s), at the end of the heating (4500s), and at the end of the cool-down (5050s).

Using a post-processing tool, the average temperature of the 18650 cylindrical cells can be evaluated and plotted versus time in terms of temperature increment compared to the initial state. The results are clearer to understand compared to the images and have been shown in **Figure 19**. The increment of temperature in the stabilized part, at the end of the heating phase, is lower for the case with the metal foams systems, presenting a reduction of 20% compared to the reference case [87].

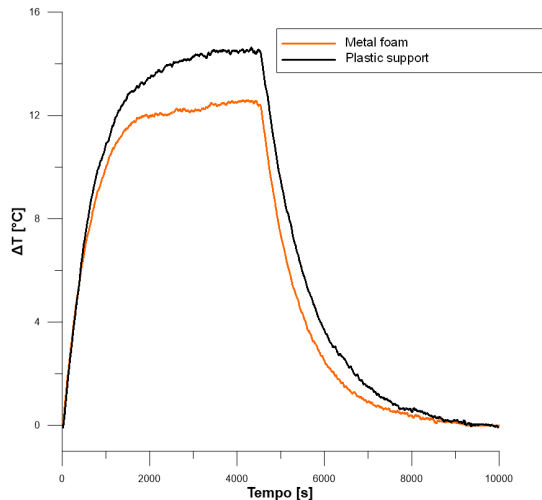


Figure 19 - Increment of temperature during the test of discharge for the three configurations with cylindrical cells and metal foam-based frame.

Finally, liquid cooling systems are a well-known technology for the management of the battery temperature. The working fluid has been deeply investigated providing a glycol-water blend as the best solution. Other research also focused on the shape of the cooling channels, testing different geometrical configurations up to investigate also a vein- or leaves-derived layouts. Here, a procedure is presented to set-up a tailored channel plate for liquid cooling based on the 3D printing procedure with plastic material [88]. The main idea is to use the printed material as insulant and the working fluid as heat dissipation mean toward the external environment. The channel plate has been designed according to the flat cell dimensions selecting an 'S'-shaped layout. The channels are covered with a 0.4 mm thickness aluminum plate that grants the heat exchange from the cell to the working fluid. The plate is accurately sealed to prevent the communication among adjacent channels. Finally, the plate is mounted on the flat cell with a 3 W/mK thermal conductivity glue. The described process can be visualized in the flow of **Figure 20**.

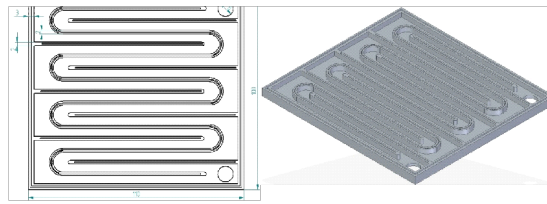


Figure 20 - Schematic of the design and production process of the 3D-printed channel plate for the flat cell.

The inlet and outlet ducts are then connected to an electric pump. Water is chosen as working fluid for simplicity because it is not the focus of the work. Some preliminary tests were made to check the sealing and the battery cooling. The 3D printed channel plate worked successfully indicating the potential of the unconventional procedure for the design of a tailored cooling system. An example of the performance of the 3D printed cooling channel is reported in **Figure 21**. The sharp increment of temperature that would occur without cooling is promptly smoothed by the cooling system, providing a difference temperature higher than 15°C after 100s of test.

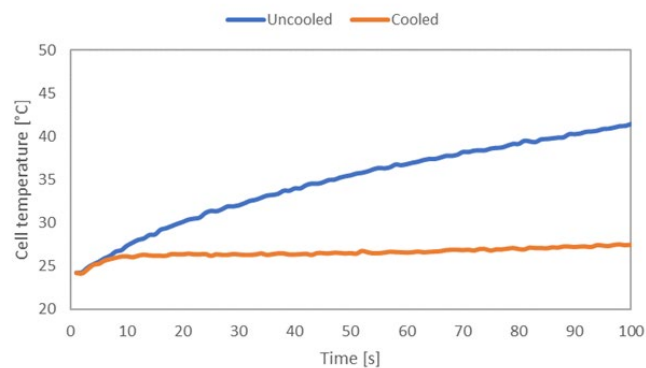


Figure 21 - Temperature variation for a discharge test with and without liquid cooling using the 3D printed channel plate.

The 3D printing technology suits very well for the planned activity, moreover, the printing material characteristics are a key parameter. The use of metal instead of plastic can be useful for the print of both cooling channels and cooling fins systems. To this purpose some market analysis has been made to find the best solution for rapid prototyping of cooling systems. Traditional metal 3D printers use lasers or electrons to melt metal powder, generating dispersed powder, radiation, and heat. This can pose a safety risk to operators and the environment.

A new innovative solution for metal parts production is a 3D printer that uses a technology that allows printing metal powder embedded in a plastic matrix. This eliminates the need for lasers or electrons, significantly reducing safety risks. The production technology is the FFF (Fused Filament Fabrication). The printer requires two accessories to complete the sample production: the wax washer, used to remove the plastic matrix from the metal parts, and the sintering furnace, to sinter the 3D washed, printed parts.

The advantages of this metal printer over the traditional metal 3D printers are the safety, as the printer does not generate dispersed powder, radiation, or heat; the reliability/accuracy of the printed metal parts; and the ease of use and maintenance. On the other hand, they are characterized by a lower print speed than traditional metal 3D printers.

1.3.4 Selection of case studies and identification of main requirements for the specific applications

The selection, implementation, and management of a proper electrochemical energy storage system for robotic devices is crucial for the safe and efficient operation of the overall system. In particular, the following factors should be carefully considered [89]:

Power demand.
 Distance to be covered and type of road surface.
 Required performance in terms of speed and acceleration.
 Weight of the payload (also by considering possible variations during working).
 Effect of the weather (e.g., increased power consumption at low or elevated temperatures).
 Required autonomy and charging opportunities.
 Battery swap capability.
 Battery chemistry with the related environmental effects.
 Volume and weight requirements.

The above factors are directly related to the main characteristics and performance parameters of the considered storage technology. In this regard, a first parameter to be considered for choosing and sizing the storage system is the *battery capacity*. This parameter is generally measured in *Ah* and can be defined as the quantity of charge that can be withdrawn, during the discharge phase, from a fully charged battery, until its minimum voltage value (cut-off voltage) is reached. It is important to note that this parameter is generally referred in the literature to the actual capacity of the battery when it is completely discharged in exactly one hour. Consequently, if a battery is characterized by a capacity of *50 Ah*, it will be fully discharged in one hour with a constant discharge current of *50 A*. On the other hand, battery manufacturers typically refer to the rated capacity at a specific discharge time, which is generally 5 h or 20 h, and report the capacity trend for different discharge current values in the form of a table or graph. The capacity values reported in the technical datasheet can be generally considered reliable only for new batteries, operating at a fixed and constant environmental temperature. The actual capacity of the battery is in fact generally influenced by the environmental parameters and the *State of Health (SoH)* of the storage system. Furthermore, the effective capacity value of a battery is generally greatly reduced for high discharge currents, due to energy losses related to incomplete or unwanted chemical reactions within individual cells. In particular, the amperometric efficiency of a storage system, also called *Coulombic efficiency*, is defined as the ratio between the Ampere-hours supplied during the charging operation and the Ampere-hours that can be withdrawn during the successive discharging operation. Similarly, *energy efficiency* can be defined by also considering the voltage values of the storage system. Specific laboratory activities can be addressed to the evaluations of the storage system capacities in different operating conditions as only a specific measurement can give a first idea of the actual values related to these performance parameters. Focusing on storage technologies, it is important to underline that Lithium battery and supercapacitor technologies generally suffer less of capacity losses in comparison with lead-acid batteries.

A rough indication of the residual energy available for the battery pack can be given by the evaluation of the *State of Charge (SoC)*. In particular, the *SoC*, at the time t_i , can be calculated with the following Equation 1

Equation 1

$$SoC(t_i) = SoC(t_0) - \frac{\int_{t_0}^{t_i} i(t) dt}{C}$$

where t_0 represents the starting time for the ESS charging/discharging operation and C is the actual capacity of the ESS. The *SoC* is generally considered for the evaluation of the remaining autonomy of an electrically supplied system. It is clear that the above equation can be considered reliable under the assumption that the value of *SoC* (t_0) and of the actual battery capacity are well known. As a matter of fact, the correct evaluation of *SoC* is generally influenced by the ambient temperature, the *SoH* of the ESS and the charge/discharge current values. For this reason, various *SoC* evaluation methods and procedures, for different storage technologies, are considered topics of particular interest for the scientific literature [90].

The capacity and *SoC* represent parameters of primary importance for the appropriate storage sizing since they are directly related to the expected autonomy of the overall system. In fact, the energy that can be stored in the battery pack depends on the capacity and is generally calculated by referring to the nominal voltage and capacity values based on Equation 2

Equation 2

$$E(Wh) = V(V) \cdot C(Ah)$$

In the case of wearable robotic applications, it is clear that the reduction of weight and dimensions represent fundamental requirements. Therefore, for these applications, as already mentioned, technologies characterized by high energy and power density values will be preferred. In particular, the *energy density* of a storage system can be defined as the electrical energy stored per unit of volume (Wh/l) or per unit of weight (Wh/kg). Volumetric energy density (Wh/l) was introduced in the past since old lead acid battery technologies were based on liquid electrolytes. However, although the application of this type of battery is not considered in the field of robotic applications, the volume of the unit is still considered useful as it can give a first idea on the size of the battery pack, useful for respecting space constraints of the considered application. Gravimetric energy density (Wh/kg) is usually referred to as *specific energy* and can be considered to evaluate the weight of a storage system. The energy density obviously impacts the autonomy of the overall robotic system since, for the same weight/size, a high energy density allows a greater quantity of energy to be stored.

Power density can be defined as the power obtainable from a storage system per unit of volume (W/l) or per unit of weight (W/kg), remaining in the allowed operative range. In the latter case, this parameter is generally referred to as *specific power*. The possibilities of supplying high peak power demand and the recharging time of a storage system directly depend on this last parameter.

From the above considerations, it is clear that, for what concerns robotic applications, the ideal condition would be to have storage systems characterized by high performance in terms of both power density and energy density.

In this regard, the current state of the technology can be resumed by the Ragone diagram shown in **Figure 22**, which compares the aforementioned parameters for different storage technologies. For example, EDLC supercapacitors have high specific power but low energy density, while lithium-ion batteries have low power density and high specific energy. Some new technologies, i.e. LIC (Lithium-ion Capacitors), on the other hand, have a power density comparable to that of super-capacitors, but greater energy density.

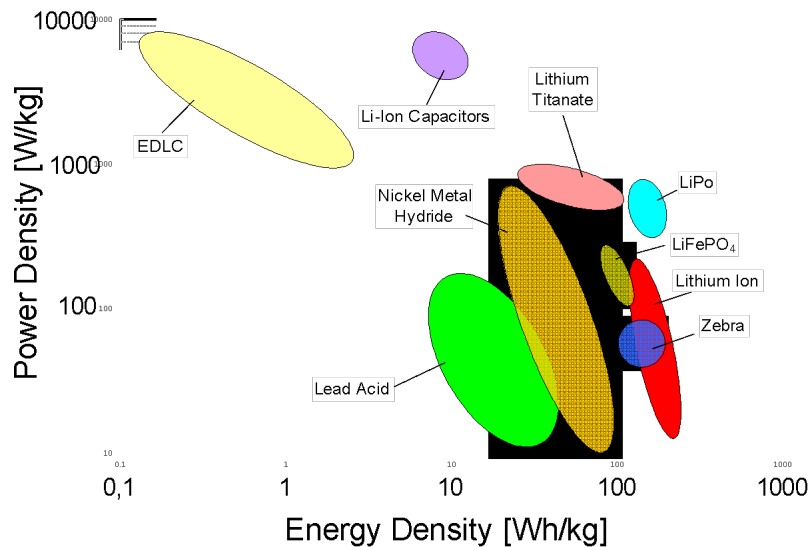


Figure 22 - Ragone Plot of Electrochemical Energy Storage Systems.

On the basis of the above evaluations it is clear that the proper choice of a storage systems mainly depends on the optimal compromise between their energy/power density, safety, cost and useful life. With particular reference to remaining useful life, storage systems performance decrease, until reaching End of Life, on the basis of calendar and cycle life. Depending on the type of application, these kinds of aging effects assume different priorities. As an example, for robotic wearable applications, which require frequent engagements of actuators, the battery pack is continuously involved in charging/discharging operations. Therefore, in these cases, cycling life becomes the reference parameter for the proper technology choice. The cyclic degradation of storage systems is defined by the number of charge/discharge cycles that an ESS can perform, without significantly reducing its effective capacity. In

general, for this parameter, actual capacity is considered acceptable until it reaches 80% of the rated capacity. The cycling life of storage systems is strongly influenced by the working temperature and the depth of discharge (DoD), which is given by the following formula for the relative evaluation time t_i :

Equation 3

$$DoD(t_i) = 100\% - SoC(t_i)$$

For this reason, battery manufacturers recommend to not exceeding the DoD value of 20% during discharge operations.

Therefore, on the basis of the definitions provided in this Section, it is clear that an ideal storage system for robotic applications must satisfy the following requirements:

- Reduced cost of both installation and maintenance.
- High reliability.
- High cycling life.
- High security.
- Safety.

In case of wearable applications High specific energy and High specific power also represent key performance parameters to be considered.

In order to resume, **Figure 42** shows the main characteristics of the different types of batteries compared via spider graphs showing: specific energy (or capacity), power, safety, efficiency, useful life and cost.

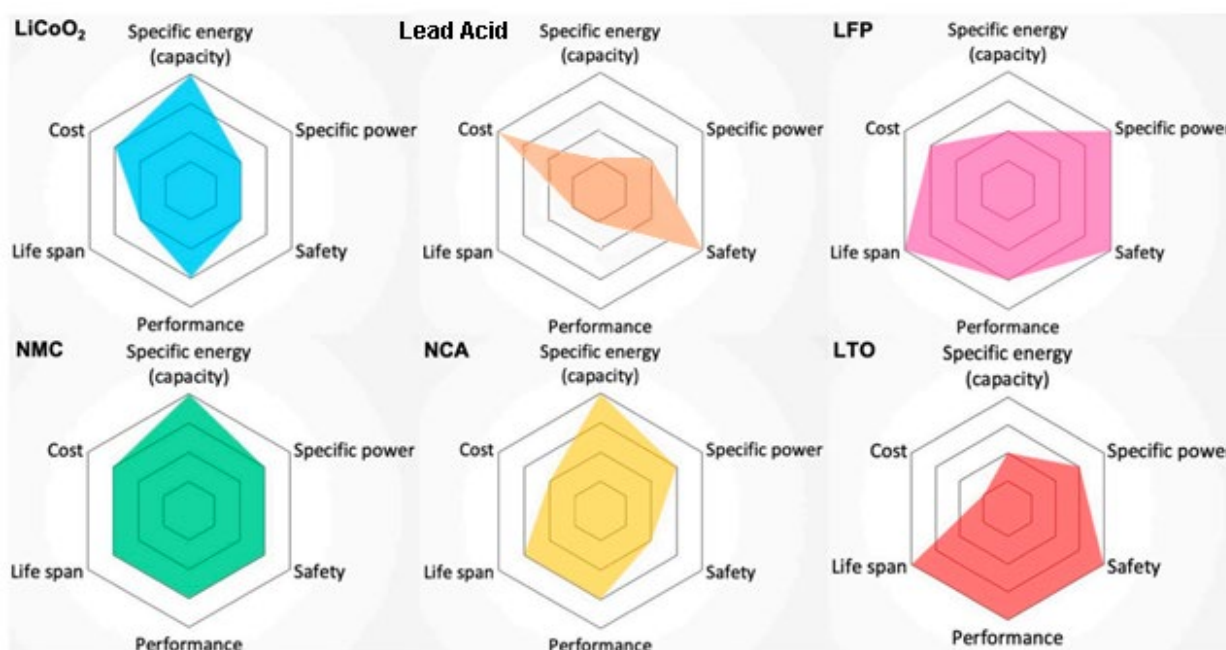


Figure 23 - Main characteristics of the analysed storage technologies.

As clearly visible, lead acid batteries present generally low performance but can be preferred in terms of safety and costs. LiCoO₂ batteries have the highest specific energy but lower specific power and relevant safety issues. Similar evaluations can be considered also valid for the NCA technology. Therefore, LFP batteries can be generally preferred for the most of robot applications, since they can be considered as an optimal trade-off between cost and performance. In case, high charging rates are required LTO batteries could represent a very attractive good solution, even though this technology is characterized by higher costs. NMC technology represents the best solution in case of mobile applications where space and weight can be considered as primary requirements.

As well-known the actual performances and behavior of energy storage systems are strongly affected by their electric and thermal operative conditions [91]. Therefore, a proper evaluation of the above parameters requires specific experimental test campaigns, to be carried out both at a single storage cell and at battery pack level. In this regard, the activities of the TEST-DEM subproject are carried out with the support of the facilities of the *Centre of Excellence on Sustainable Energies Sources (CoE-SES)*, to be completed in the framework of the Fit4Med Project. In particular, on-going activities are focused on the set-up of the laboratory test benches with specific devices completely devoted to experimental analysis and characterization of storage systems from both electric and thermal points of view.

In particular, the laboratory bench for electric tests on a single storage cell is based on a controlled DC power supply, working in combination with an electronic DC load. The functional scheme is reported in the following **Figure 24**.

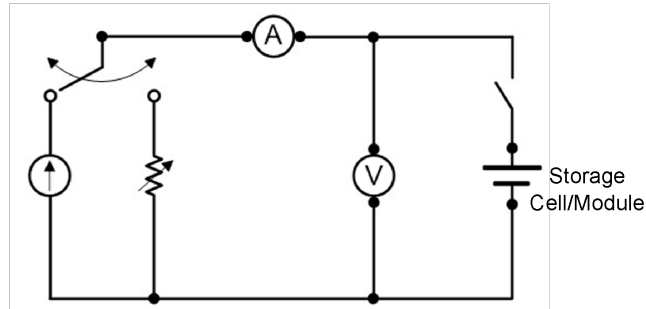


Figure 24 - Functional scheme of the electric test bench.

A more efficient testing solution can be obtained by using active bidirectional power suppliers, where the storage cell/module under test can be directly discharged feeding electric power back to the main grid. As a matter of fact, specific experimental analyses generally involve long testing times and need to be repeated on a different number of cells characterized by the same chemistry and technology. Therefore, in the context of the TEST-DEM sub-project, the requirements of a specific device for multi-cell/module tests have been defined, considering the main characteristics of the storage technologies to be experimentally tested and characterized. In particular, at this stage, an Expression of Interest (EoI) procedure has been published in order to collect and compare the quotations received from different suppliers.

The main characteristics required for the above system are reported in the following **Table 5**.

Table 5 - Main characteristic of the multi-channel cell/module storage tester.

Minimum number of channels	5
Power architecture of each channel	Based on bidirectional power converters
Maximum power value for each channel	± 6 kW
Maximum current value for each channel	± 240 A
Maximum Voltage Value at Maximum current	70% (V_{fs})
Operative Voltage range at Maximum current in power supplier mode	0 - V_{fs}
Operative Voltage range at Maximum current in DC load mode	$0.5 \div V_{fs}$
Overall Maximum Current	5 x 240 A through channels' parallel options
Software	Dedicated software for the management of a minimum number of 10 parallel tests
Remote Interfaces	RS232, analog interface
Temperature Scanner	10-channel temperature scanner system
Internal Resistance (IR) Scanner	10-channel IR scanner system

The acquisition & control system of the laboratory test bench is based on a National Instruments CompactRIO device equipped with voltage, current, temperature modules. In this regard, a software interface has been realized in the Labview environment to monitor cell behavior during the test and to store all the experimental data for the required analysis.

The surface temperature of the battery can be monitored with contact and contactless techniques. An infrared camera is available in the laboratory of STEMS. For the detection of the 2d temperature distribution it must be placed in front of the battery to detect thermal radiation through the inspection access of a testing box where the battery is placed. The camera has a resolution of 320×256 pixels and is sensitive in the range of $3.0\text{--}5.5 \mu\text{m}$. It has a sensor made of Indium Antimonide. The acquisition frequency can be set according to the application while an exposure time of $260 \mu\text{s}$ provides the best compromise between recording quality and image saturation when low temperature values ($20^\circ\text{C}\text{--}25^\circ\text{C}$) must be recorded. The Noise Equivalent Temperature Difference (NETD) of the camera corresponds to the standard deviation of the temperature distribution, for the present camera it is 0.1°C . Hence, an error of $\pm 0.1^\circ\text{C}$ is considered for the infrared temperature measurements. On the other hand, the contact method consists of a K-type thermocouple installed on the battery surface. The thermocouple has a sensitivity of 0.5°C ; its signal is managed and recorded with an I/O analog module and a homemade acquisition interface. A temperature-humidity sensor is placed in the test box to monitor the ambient conditions. These two temperature sensors (thermocouple and ambient sensors) are used to check and calibrate the signal of the camera before each test in steady conditions. The temperature of the battery and the background detected by the thermal camera is compared to the measured ones. This allows setting the correct value of emissivity for the evaluation of the temperature variation during the test with the infrared technique. Also, to avoid reflections, the battery is covered with rough tape while the test box is black painted with opaque paint. The complete layout is shown in **Figure 25**.

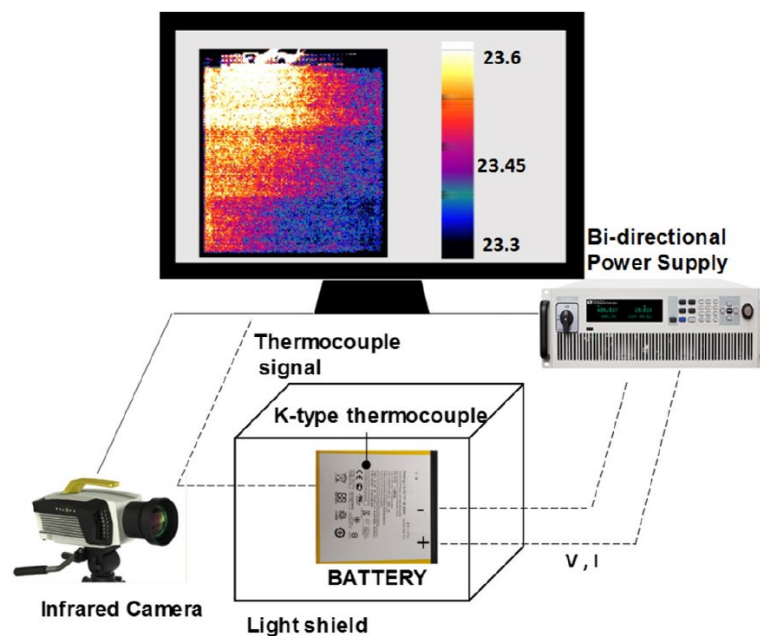


Figure 25 - The layout of the experimental setup and a sequence of 5 infrared images of the battery recorded by the thermal camera.

As the last part of the activities described in this Section, a case study based on an example of wearable exoskeleton robot has been analysed for preliminary evaluations. In particular, picture and hierarchical control scheme of the considered application is reported in **Figure 26**.

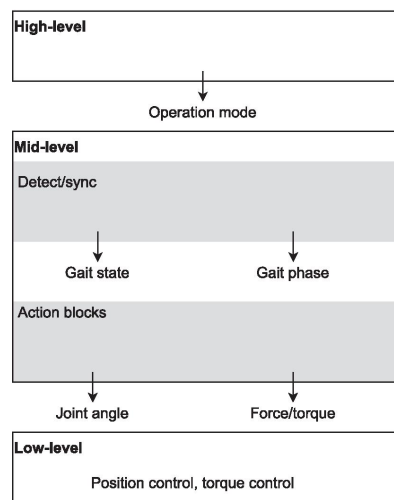


Figure 26 - Picture and control scheme of the considered exoskeleton (Source: [56]).

The high-level control defines the general behavior of the exoskeleton on the basis of the desired operative conditions (e.g. walking, climbing stairs, sitting). The mid-level defines the continuous behavior of the robot, following, on the basis of user interactions, reference joints target torque or position, at each timestep of the main control loop. The low level is directly involved in position and torque control through the proper interaction with the actuators. As a matter of fact, electric power required to supply control and sensing devices represent just a small percentage of the overall system power demand, and its operative profile is generally characterized by an almost constant behavior. On the other hand, the greatest amount of electric power is required to supply motors/actuators during the various system operations. In this regard, **Figure 27** reports the Current vs Time profile of the wearable exoskeleton robot, for human gait support, during its main operations.

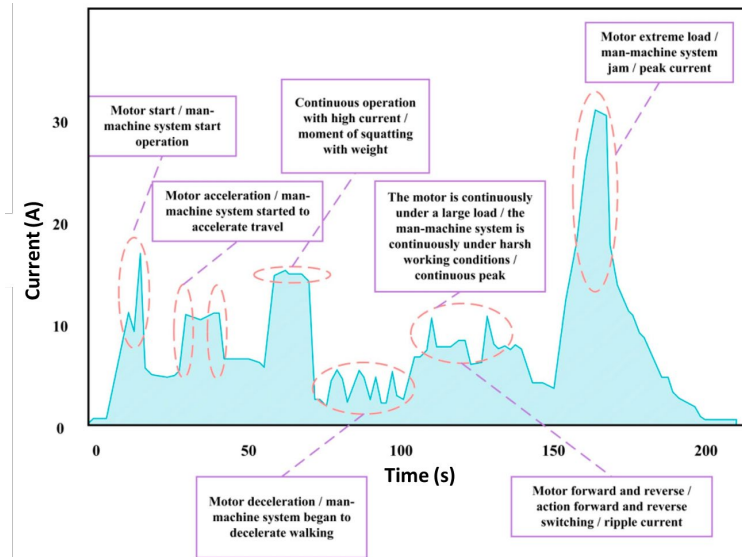


Figure 27 - Current vs Time behaviour for a wearable exoskeleton robot (Source: [57]).

In this case, the power required for the operations of the overall system (human + exoskeleton), P_t , can be evaluated by considering the power coming from the human, P_h , and from the exoskeleton, P_e , by means of the following equation:

$$P_t = P_h + P_e = P_h + P_e^a + P_e^p$$

where P_e^a and P_e^p respectively represent the active and passive power provided by the exoskeleton to support human incoordination.

Since the considered exoskeleton represents a mobile robotic application, a specific energy storage system needs to be properly considered, with the related management technology and strategy. In particular, as clearly observable from the profile of **Figure 27**, the current behavior of the exoskeleton is characterized by low average values and frequent fast transient operations, involving high peak current values. These peak values can be mainly related to motors' engagement and extreme load conditions. As reported in the literature [92], [93], transient peak power operations negatively affect battery cycle life, thereby increasing overall system maintenance costs. One possible solution is the combined use of two different storage technologies (i.e. supercapacitors and batteries) in hybrid energy storage system configurations. The integration of the above storage technologies can be performed by using a DC/DC power converter as reported in the following **Figure 28**.

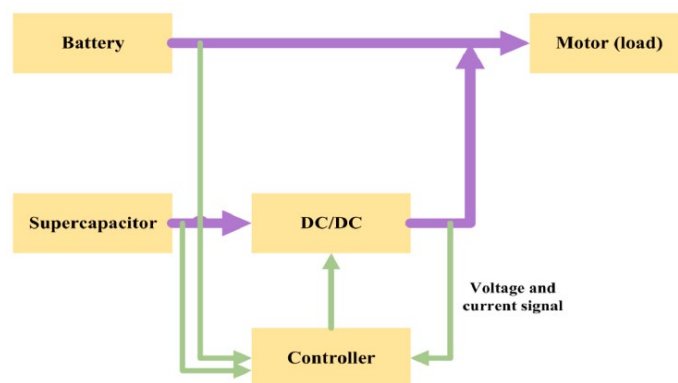


Figure 28 - Hybrid energy storage architecture (Source: [94]).

In this case, the power converter can be used to manage power flows between battery and supercapacitors by reducing battery peak current and resulting in smoother battery current profiles.

REFERENCES

- [1] C. Lee *et al.*, «Soft robot review», *Int. J. Control Autom. Syst.*, vol. 15, pp. 3–15, 2017.
- [2] H. Wang, M. Totaro, e L. Beccai, «Toward perceptive soft robots: Progress and challenges», *Adv. Sci.*, vol. 5, fasc. 9, p. 1800541, 2018.
- [3] Y. Sun, Y. S. Song, e J. Paik, «Characterization of silicone rubber based soft pneumatic actuators», in *2013 IEEE/RSJ International Conference on Intelligent Robots and Systems*, Ieee, 2013, pp. 4446–4453.
- [4] Y. Yamamoto, K. Kure, T. Iwa, T. Kanda, e K. Suzumori, «Proc. of the 2007 IEEE/RSJ IROS», 2007.
- [5] S. Cheng, Y. S. Narang, C. Yang, Z. Suo, e R. D. Howe, «Stick-on large-strain sensors for soft robots», *Adv. Mater. Interfaces*, vol. 6, fasc. 20, p. 1900985, 2019.
- [6] H. Zhao, K. O'brien, S. Li, e R. F. Shepherd, «Optoelectronically innervated soft prosthetic hand via stretchable optical waveguides», *Sci. Robot.*, vol. 1, fasc. 1, p. eaai7529, 2016.
- [7] V. R. Marrazzo, F. Fienga, M. Riccio, A. Irace, e G. Breglio, «Multichannel approach for arrayed waveguide grating-based fbg interrogation systems», *Sensors*, vol. 21, fasc. 18, p. 6214, 2021.
- [8] D. Prattichizzo *et al.*, «Human augmentation by wearable supernumerary robotic limbs: review and perspectives», *Prog. Biomed. Eng.*, vol. 3, fasc. 4, p. 042005, 2021.
- [9] S. Uran e J. Geršak, «Smart clothing to increase safety of people with dementia», in *IOP Conference Series: Materials Science and Engineering*, IOP Publishing, 2018, p. 012047.
- [10] M. Chessa, S. P. Sabatini, e F. Solari, «A fast joint bioinspired algorithm for optic flow and two-dimensional disparity estimation», in *Computer Vision Systems: 7th International Conference on Computer Vision Systems, ICVS 2009 Liège, Belgium, October 13-15, 2009. Proceedings 7*, Springer, 2009, pp. 184–193.
- [11] M. Ferrari, L. Mottola, e V. Quaresima, «Principles, techniques, and limitations of near infrared spectroscopy», *Can. J. Appl. Physiol.*, vol. 29, fasc. 4, pp. 463–487, 2004.
- [12] M. Paleari, R. Luciani, e P. Ariano, «Towards NIRS-based hand movement recognition», in *2017 International Conference on Rehabilitation Robotics (ICORR)*, IEEE, 2017, pp. 1506–1511.
- [13] P. Fitzpatrick, A. Needham, L. Natale, e G. Metta, «Shared challenges in object perception for robots and infants», *Infant Child Dev. Int. J. Res. Pract.*, vol. 17, fasc. 1, pp. 7–24, 2008.
- [14] S. Fuke, M. Ogino, e M. Asada, «Acquisition of the head-centered peri-personal spatial representation found in vip neuron», *IEEE Trans. Auton. Ment. Dev.*, vol. 1, fasc. 2, pp. 131–140, 2009.
- [15] Y. Mansouri e M. A. Babar, «A review of edge computing: Features and resource virtualization», *J. Parallel Distrib. Comput.*, vol. 150, pp. 155–183, 2021.
- [16] S. Goure e S. Banu, «A comprehensive review on edge computing», *IJRASET*, vol. 11, fasc. 1, pp. 92–106, 2023.
- [17] A. Bourechak, O. Zedadra, M. N. Kouahla, A. Guerrieri, H. Seridi, e G. Fortino, «At the Confluence of Artificial Intelligence and Edge Computing in IoT-Based Applications: A Review and New Perspectives», *Sensors*, vol. 23, fasc. 3, p. 1639, 2023.
- [18] M. S. Graziano, «Where is my arm? The relative role of vision and proprioception in the neuronal representation of limb position», *Proc. Natl. Acad. Sci.*, vol. 96, fasc. 18, pp. 10418–10421, 1999.
- [19] S. Wolf *et al.*, «Variable stiffness actuators: Review on design and components», *IEEEASME Trans. Mechatron.*, vol. 21, fasc. 5, pp. 2418–2430, 2015.
- [20] R. Ham, T. Sugar, B. Vanderborght, K. Hollander, e D. Lefeber, «Compliant actuator designs», *IEEE Robot. Autom. Mag.*, vol. 3, fasc. 16, pp. 81–94, 2009.
- [21] K. Kalou, G. Sedda, A. Gibaldi, e S. P. Sabatini, «Learning bio-inspired head-centric representations of 3D shapes in an active fixation setting», *Front. Robot. AI*, vol. 9, p. 994284, 2022.
- [22] L. Fogassi, V. Gallese, L. Fadiga, G. Luppino, M. Matelli, e G. Rizzolatti, «Coding of peripersonal space in inferior premotor cortex (area F4)», *J. Neurophysiol.*, vol. 76, fasc. 1, pp. 141–157, 1996.
- [23] B. Vanderborght *et al.*, «Variable impedance actuators: A review», *Robot. Auton. Syst.*, vol. 61, fasc. 12, pp. 1601–1614, 2013.
- [24] S. A. Migliore, E. A. Brown, e S. P. DeWeerth, «Biologically inspired joint stiffness control», in *Proceedings of the 2005 IEEE international conference on robotics and automation*, IEEE, 2005, pp. 4508–4513.
- [25] I. Sardellitti, G. Palli, N. G. Tsagarakis, e D. G. Caldwell, «Antagonistically actuated compliant joint: Torque and stiffness control», in *2010 IEEE/RSJ International Conference on Intelligent Robots and Systems*, IEEE, 2010, pp. 1909–1914.

- [26] F. Cordella *et al.*, «Literature review on needs of upper limb prosthesis users», *Front. Neurosci.*, vol. 10, p. 209, 2016.
- [27] P. Bilancia, G. Berselli, e G. Palli, «Virtual and physical prototyping of a beam-based variable stiffness actuator for safe human-machine interaction», *Robot. Comput.-Integr. Manuf.*, vol. 65, p. 101886, 2020.
- [28] M. del C. Sanchez-Villamañan, J. Gonzalez-Vargas, D. Torricelli, J. C. Moreno, e J. L. Pons, «Compliant lower limb exoskeletons: a comprehensive review on mechanical design principles», *J. Neuroengineering Rehabil.*, vol. 16, fasc. 1, pp. 1–16, 2019.
- [29] G. A. Pratt e M. M. Williamson, «Series elastic actuators», in *Proceedings 1995 IEEE/RSJ International Conference on Intelligent Robots and Systems. Human Robot Interaction and Cooperative Robots*, IEEE, 1995, pp. 399–406.
- [30] D. W. Robinson, «Design and analysis of series elasticity in closed-loop actuator force control», PhD Thesis, Massachusetts Institute of Technology, 2000.
- [31] G. Carpino, D. Accoto, F. Sergi, N. Luigi Tagliamonte, e E. Guglielmelli, «A novel compact torsional spring for series elastic actuators for assistive wearable robots», *J. Mech. Des.*, vol. 134, fasc. 12, p. 121002, 2012.
- [32] D. Paluska e H. Herr, «The effect of series elasticity on actuator power and work output: Implications for robotic and prosthetic joint design», *Robot. Auton. Syst.*, vol. 54, fasc. 8, pp. 667–673, 2006.
- [33] O. S. Al-Dahiree, R. A. R. Ghazilla, M. O. Tokhi, H. J. Yap, e M. Gul, «Design and Characterization of a Low-Cost and Efficient Torsional Spring for ES-RSEA», *Sensors*, vol. 23, fasc. 7, p. 3705, 2023.
- [34] J. Hurst, A. Rizzi, e D. Hobbelen, «Series elastic actuation: Potential and pitfalls», in *International conference on climbing and walking robots*, 2004.
- [35] J. P. Cummings, D. Ruiken, E. L. Wilkinson, M. W. Lanighan, R. A. Grupen, e F. C. Sup IV, «A compact, modular series elastic actuator», *J. Mech. Robot.*, vol. 8, fasc. 4, p. 041016, 2016.
- [36] J. Pratt e B. Krupp, «Series elastic actuators for legged robots», *Unmanned Ground Vehicle Technology VI*, pp. 135–144, 2004.
- [37] A. Calanca, R. Muradore, e P. Fiorini, «A review of algorithms for compliant control of stiff and fixed-compliance robots», *IEEEASME Trans. Mechatron.*, vol. 21, fasc. 2, pp. 613–624, 2015.
- [38] J. Zhang e S. H. Collins, «The passive series stiffness that optimizes torque tracking for a lower-limb exoskeleton in human walking», *Front. Neurobotics*, vol. 11, p. 68, 2017.
- [39] S. Wang *et al.*, «Design and control of the MINDWALKER exoskeleton», *IEEE Trans. Neural Syst. Rehabil. Eng.*, vol. 23, fasc. 2, pp. 277–286, 2014.
- [40] G. Chen, P. Qi, Z. Guo, e H. Yu, «Mechanical design and evaluation of a compact portable knee–ankle–foot robot for gait rehabilitation», *Mech. Mach. Theory*, vol. 103, pp. 51–64, 2016.
- [41] C. Zhang, Y. Zhu, J. Fan, J. Zhao, e H. Yu, «Design of a quasi-passive 3 DOFs ankle-foot wearable rehabilitation orthosis», *Biomed. Mater. Eng.*, vol. 26, fasc. s1, pp. S647–S654, 2015.
- [42] C. Lagoda, A. Schouten, E. Hekman, e H. van Der Kooij, «Design of an electric series elastic actuated joint for robotic gait rehabilitation training», *3rd IEEE RAS & EMBS International Conference on Biomedical Robotics and Biomechatronics (BioRob)*, 2010.
- [43] T. Bacek, R. Unal, K. Junius, H. Cuyppers, e B. Vanderborght, «Conceptual Design of a Novel Variable Stiffness Actuator for Use in Lower Limb Exoskeletons», *2015 IEEE International Conference on Rehabilitation Robotics (ICORR)*, Singapore, 2015.
- [44] P. Agarwal e A. Deshpande, «Series elastic actuators for small-scale robotic applications», *Journal of Mechanisms and Robotics*, 9(3), 2017.
- [45] J. Veneman, R. Ekkelenkamp, R. Kruidhof, F. van der Helm, e H. van Der Kooij, «A Series Elastic- and Bowden-Cable-Based Actuation System for Use as Torque Actuator in Exoskeleton-Type Robots», *Int. J. Rob. Res.*, pp. 261–281, 2006.
- [46] G. Wyeth, «Demonstrating the Safety and Performance of a Velocity Sourced Series Elastic Actuator», *Proceedings of IEEE International Conference on Robotics and Automation*, pp. 3642–3647, 2008.
- [47] N. G. Tsagarakis, M. Laffrachi, B. Vanderborght, e D. G. Caldwell, «A Compact Soft Actuator Unit for Small Scale Human Friendly Robots», *Proceedings of IEEE International Conference on Robotics and Automation*, pp. 4356–4362, 2009.
- [48] S. Yoon, S. Kang, S. Kim, Y. Kim, M. Kim, e C. Lee, «Safe Arm With MR-Based Passive Compliant Joints and Visco-Elastic Covering for Service Robot Applications», *Proceedings of IEEE/RSJ International Conference on Intelligent Robots and Systems*, pp. 2191–2196., 2003.

- [49] G. Wyeth, «Control Issues for Velocity Sourced Series Elastic Actuators», *Proceedings of Australasian Conference on Robotics and Automation.*, 2006.
- [50] B. Celebi, M. Yalcin, e V. Patoglu, «AssistOn-Knee: A self-aligning knee exoskeleton», *2013 IEEE/RSJ International Conference on Intelligent Robots and Systems. IEEE.*, pp. 996–1002, 2013.
- [51] K. Kong, J. Bae, e M. Tomizuka, «A Compact Rotary Series Elastic Actuator for Knee Joint Assistive System», *Proceedings of 2010 IEEE International Conference on Robotics and Automation*, pp. 2940–2945, 2010.
- [52] C. Lee e S. Oh, «Development, analysis, and control of series elastic actuator-driven robot leg», *Frontiers in neurorobotics*, 13, 17, 2019.
- [53] J. Sulzer, «A highly backdrivable, lightweight knee actuator for investigating gait in stroke», *IEEE Transactions on Robotics*, 25(3), 539-548, 2009.
- [54] B. Knox e J. Schriedeler, «A Unidirectional Series-Elastic Actuator Design Using a Spiral Torsion Spring», *SME J. Mech. Des.*, pp. 1–5, 2009.
- [55] W. Choi, J. Won, J. Lee, e J. Park, «Low stiffness design and hysteresis compensation torque control of SEA for active exercise rehabilitation robots», *Auton Robots*, pp. 1221–42, 2017.
- [56] O. S. Al-Dahiree, R. A. R. Ghazilla, M. O. Tokhi, H. J. Yap, e E. Albaadani, «Design of a compact energy storage with rotary series elastic actuator for lumbar support exoskeleton», *Machines*, 10(7), 584, 2022.
- [57] M. Cempini *et al.*, «NEUROExos: A powered elbow orthosis for post-stroke early neurorehabilitation», *2013 35th Annual International Conference of the IEEE Engineering in Medicine and Biology Society (EMBC).*, pp. 342–345, 2013.
- [58] D. Accoto, G. Carpino, F. Sergi, L. Zollo, e E. Guglielmelli, «Design and characterization of a novel high-power series elastic actuator for a lower limb robotic orthosis», *Int J Adv Robot Syst.*, 2013.
- [59] A. Stienen, E. Hekman, H. Braak, A. Aalsma, F. van der Helm, e H. van Der Kooij, «Design of a Rotational Hydroelastic Actuator for a Powered Exoskeleton for Upper Limb Rehabilitation», *IEEE Trans. Biomed. Eng.*, 57(3), pp. 728–735, 2010.
- [60] C. Irmscher, E. Woschke, E. May, e C. Daniel, «Design, optimisation and testing of a compact, inexpensive elastic element for series elastic actuators», *Med Eng Phys*, pp. 84–89, 2017.
- [61] W. dos Santos, G. Caurin, e A. Siqueira, «Design and control of an active knee orthosis driven by a rotary Series Elastic Actuator», *Control Eng. Practice*, pp. 307–318, 2017.
- [62] N. Paine *et al.*, «Actuator Control for the NASA-JSC Valkyrie Humanoid Robot: A Decoupled Dynamics Approach for Torque Control of Series Elastic Robots», *J. Field Robotics*, pp. 378–396.
- [63] S. Zhang, Q. Zhu, J. Wu, R. Xiong, e Y. Gu, «Design and compliance control of rehabilitation exoskeleton for elbow joint ankylosis», in *2020 IEEE/ASME International Conference on Advanced Intelligent Mechatronics (AIM)*, IEEE, 2020, pp. 1896–1901.
- [64] L. Wang, Z. Du, W. Dong, Y. Shen, e G. Zhao, «Intrinsic sensing and evolving internal model control of compact elastic module for a lower extremity exoskeleton», *Sensors*, vol. 18, fasc. 3, p. 909, 2018.
- [65] M. C. Yildirim *et al.*, «Design and development of a durable series elastic actuator with an optimized spring topology», *Proc. Inst. Mech. Eng. Part C J. Mech. Eng. Sci.*, vol. 235, fasc. 24, pp. 7848–7858, 2021.
- [66] T. Zhang, M. Tran, e H. Huang, «Admittance shaping-based assistive control of SEA-driven robotic hip exoskeleton», *IEEE/ASME Trans. Mechatron.*, vol. 24, fasc. 4, pp. 1508–1519, 2019.
- [67] F. Lopes e M. Meggiolaro, «Design of a Low-Cost Series Elastic Actuator for Application in Robotic Manipulators», in *26th International Congress of Mechanical Engineering-COBEM2021*, 2021.
- [68] H. İ. Erten, «Optimum design and analysis of torsion spring used in series elastic actuators for rehabilitation robots», Master's Thesis, Izmir Institute of Technology, 2021.
- [69] Y. Chen, Y. Huang, K. Chen, Y. Wang, e Y. Wu, «Novel torsional spring with corrugated flexible units for series elastic actuators for cooperative robots», *J. Mech. Sci. Technol.*, vol. 36, fasc. 6, pp. 3131–3142, 2022.
- [70] Y. Wang, Y. Chen, K. Chen, Y. Wu, e Y. Huang, «A flat torsional spring with corrugated flexible units for series elastic actuators», in *2017 2nd International Conference on Advanced Robotics and Mechatronics (ICARM)*, IEEE, 2017, pp. 138–143.
- [71] G. Carabin, E. Wehrle, e R. Vidoni, «A review on energy-saving optimization methods for robotic and automatic systems», *Robotics*, vol. 6, fasc. 4, p. 39, 2017.
- [72] G. J. May, A. Davidson, e B. Monahov, «Lead batteries for utility energy storage: A review», *J. Energy Storage*, vol. 15, pp. 145–157, 2018.

- [73] «Panasonic Autonomous Delivery Robots - HOSPI - Aid Hospital Operations at Changi General Hospital. Available at: <https://news.panasonic.com/global/topics/4923>».
- [74] D. J. Garole, R. Hossain, V. J. Garole, V. Sahajwalla, J. Nerkar, e D. P. Dubal, «Recycle, recover and repurpose strategy of Spent Li-ion Batteries and catalysts: current status and future opportunities», *ChemSusChem*, vol. 13, fasc. 12, pp. 3079–3100, 2020.
- [75] Y. Miao, P. Hyman, A. Von Jouanne, e A. Yokochi, «Current Li-ion battery technologies in electric vehicles and opportunities for advancements», *Energies*, vol. 12, fasc. 6, p. 1074, 2019.
- [76] B. Scrosati e J. Garche, «Lithium batteries: Status, prospects and future», *J. Power Sources*, vol. 195, fasc. 9, pp. 2419–2430, 2010.
- [77] C. Capasso e O. Veneri, «Experimental analysis on the performance of lithium based batteries for road full electric and hybrid vehicles», *Appl. Energy*, vol. 136, pp. 921–930, 2014.
- [78] «IAM Robotics Takes on Automated Warehouse Picking. Available at: <https://spectrum.ieee.org/iam-robotics-takes-on-automated-warehouse-picking>».
- [79] «Reeman Disinfection Robot. available at: <https://www.reemanrobot.com/disinfection-robot/>».
- [80] O. Veneri, L. Ferraro, C. Capasso, e D. Iannuzzi, «Charging infrastructures for EV: Overview of technologies and issues», *2012 Electr. Syst. Aircr. Railw. Ship Propuls.*, pp. 1–6, 2012.
- [81] «Lithium Titanate Batteries Market (By Type: 15-1000mAh, 1000-5000mAh, 5000-10000mAh, Others; By Application: EV, HEV, Others) - Global Industry Analysis, Size, Share, Growth, Trends, Regional Outlook, and Forecast 2023-2032. Available at: <https://www.precedenceresearch.com/lithium-titanate-batteries-market>».
- [82] «Battery Packs for Portable Medical Equipment. available at: <https://greencubes.com/applications/mobile/portable-medical-equipment/>», *Green cubes*.
- [83] D. McNulty, A. Hennessy, M. Li, E. Armstrong, e K. M. Ryan, «A review of Li-ion batteries for autonomous mobile robots: Perspectives and outlook for the future», *J. Power Sources*, vol. 545, p. 231943, 2022.
- [84] L. Sequino, G. Sebastianelli, e B. M. Vaglieco, «Carbon and Graphene Coatings for the Thermal Management of Sustainable LMP Batteries for Automotive Applications», *Materials*, vol. 15, fasc. 21, p. 7744, 2022.
- [85] L. Sequino, G. Sebastianelli, e B. M. Vaglieco, «Measurements and Modeling of the Temperature of a Li-polymer Battery Provided with Different Coatings for Heat Dissipation», SAE Technical Paper, 2022.
- [86] L. Sequino e B. Vaglieco, «An empirical study for the correction of the thermal parameters of a Li–Po battery with carbon-graphene-silicone coatings», *Case Stud. Therm. Eng.*, vol. 45, p. 102955, 2023.
- [87] L. Sequino, C. Capasso, G. Costanza, e M. E. Tata, «Experimental Investigation on Thermal Effects of a Metal Foam-based Frame Application for Lithium-Ion Cells», SAE Technical Paper, 2023.
- [88] T. Castiglione, D. Perrone, D. La Gamba, S. Bova, L. Sequino, e B. M. Vaglieco, «Numerical Modelling and Experimental Validation of the Thermal Behavior of Li-ion Batteries for EVs Applications», SAE Technical Paper, 2023.
- [89] T. Mikołajczyk *et al.*, «Energy Sources of Mobile Robot Power Systems: A Systematic Review and Comparison of Efficiency», *Appl. Sci.*, vol. 13, fasc. 13, p. 7547, 2023.
- [90] M. A. Hannan, M. H. Lipu, A. Hussain, e A. Mohamed, «A review of lithium-ion battery state of charge estimation and management system in electric vehicle applications: Challenges and recommendations», *Renew. Sustain. Energy Rev.*, vol. 78, pp. 834–854, 2017.
- [91] W. Zichen e D. Changqing, «A comprehensive review on thermal management systems for power lithium-ion batteries», *Renew. Sustain. Energy Rev.*, vol. 139, p. 110685, 2021.
- [92] E. Wood, M. Alexander, e T. H. Bradley, «Investigation of battery end-of-life conditions for plug-in hybrid electric vehicles», *J. Power Sources*, vol. 196, fasc. 11, pp. 5147–5154, 2011.
- [93] K. Smith, M. Earleywine, E. Wood, J. Neubauer, e A. Pesaran, «Comparison of plug-in hybrid electric vehicle battery life across geographies and drive-cycles», National Renewable Energy Lab.(NREL), Golden, CO (United States), 2012.
- [94] J. Li e C. Chen, «Machine learning-based energy harvesting for wearable exoskeleton robots», *Sustainable Energy Technologies and Assessments*, 2023.